

1 Actual evapotranspiration and precipitation measured by
2 lysimeters: A comparison with eddy covariance and tipping
3 bucket

4 **S. Gebler¹, H.-J. Hendricks Franssen¹, T. Pütz¹, H. Post¹, M. Schmidt¹, H. Vereecken¹**

5 [1] Agrosphere Institute (IBG-3), Forschungszentrum Jülich, 52425 Jülich, Germany

6 Correspondence to: S. Gebler (s.gebler@fz-juelich.de)

7

8 **Abstract**

9 This study compares actual evapotranspiration (ET_a) measurements by a set of six weighable
10 lysimeters, ET_a estimates obtained with the eddy covariance (EC) method, and evapotranspiration
11 calculated with the full-form Penman-Monteith equation (ET_{PM}) for the Rollesbroich site in the
12 Eifel (Western Germany). The comparison of ET_a measured by EC (including correction of the
13 energy balance deficit) and by lysimeters is rarely reported in literature and allows more insight
14 into the performance of both methods. An evaluation of ET_a for the two methods for the year
15 2012 shows a good agreement with a total difference of 3.8 % (19 mm) between the ET_a
16 estimates. The highest agreement and smallest relative differences (< 8 %) on monthly basis
17 between both methods are found in summer. ET_a was close to ET_{PM} , indicating that ET was
18 energy limited and not limited by water availability. ET_a differences between lysimeter and EC
19 were mainly related to differences in grass height caused by harvest and the EC footprint. The
20 lysimeter data were also used to estimate precipitation amounts in combination with a filter
21 algorithm for high precision lysimeters recently introduced by Peters et al. (2014). The estimated
22 precipitation amounts from the lysimeter data differ significantly from precipitation amounts
23 recorded with a standard rain gauge at the Rollesbroich test site. For the complete year 2012 the
24 lysimeter records show a 16 % higher precipitation amount than the tipping bucket. After a
25 correction of the tipping bucket measurements by the method of Richter (1995) this amount was
26 reduced to 3 %. With the help of an on-site camera the precipitation measurements of the
27 lysimeters were analyzed in more detail. It was found that the lysimeters record more
28 precipitation than the tipping bucket in part related to the detection of rime and dew, which
29 contributes 17 % to the yearly difference between both methods. In addition, fog and drizzle
30 explain an additional 5.5 % of the total difference. Larger differences are also recorded for snow
31 and sleet situations. During snowfall, the tipping bucket device underestimated precipitation
32 severely and these situations contributed also 7.9 % to the total difference. However, 36% of the
33 total yearly difference was associated to snow cover without apparent snowfall and under these
34 conditions snow bridges and snow drift seem to explain the strong overestimation of precipitation
35 by the lysimeter. The remaining precipitation difference (about 33 %) could not be explained, and
36 did not show a clear relation with wind speed. The variation of the individual lysimeters devices
37 compared to the lysimeter mean are small showing variations up to 3 % for precipitation and 8 %
38 for evapotranspiration.

39 1. Introduction

40 Precise estimates of precipitation and actual evapotranspiration are important for an improved
41 understanding of water and energy exchange processes between land and atmosphere relevant for
42 many scientific disciplines and agricultural management. Information about measurement errors
43 and uncertainties is essential for improving measurement methods and correction techniques as
44 well as for dealing with uncertainty during calibration and validation of model simulations.
45 Although first devices for modern scientific purposes were developed in Europe during the 17th
46 century (Kohnke et al., 1940; Strangeways, 2010), the accurate estimation of precipitation (P)
47 and actual evapotranspiration (ET_a) is still a challenge. Common precipitation measurement
48 methods exhibit systematic and random errors depending on the device locations and climatic
49 conditions. Legates and DeLiberty (1993) concluded from their long-term study of precipitation
50 biases in the United States that Hellman type gauges (US standard) undercatch precipitation
51 amounts. Undercatch is larger in case of snowfall and larger wind speeds. Wind-induced loss is
52 seen as the main source of error (Sevruk, 1981 & 1996; Yang et al., 1998; Chvíla et al., 2005;
53 Brutsaert, 2010). Precipitation gauges are commonly installed above ground to avoid negative
54 impact on the measurements by splash water, hail, and snow drift. However, this common gauge
55 setup causes wind distortion and promotes the development of eddies around the device. Wind
56 tunnel experiments with Hellman type gauges (Nešpor and Sevruk, 1999) have shown
57 precipitation losses of 2 – 10 % for rain and 20 – 50 % for snow compared to the preset
58 precipitation amount. In general, wind-induced loss increases with installation height of the
59 device and wind speed and decreases with precipitation intensity (Sevruk, 1989). Intercomparison
60 studies between different rain gauge designs of the World Meteorological Organization (WMO)
61 indicated that shielded devices can considerably reduce this undercatch compared to unshielded
62 gauges, in particular for snow and mixed precipitation (Goodison et al., 1997). Further
63 precipitation losses, which affect the rain gauge measurement, are evaporation of water from the
64 gauge surface and recording mechanisms (Sevruk, 1981; Michelson, 2004). Moreover,
65 measurement methods (e.g. condensation plates, optical methods) to estimate the contribution of
66 rime, dew and fog to the total precipitation, exhibit a high uncertainty (Jacobs et al., 2006). A
67 short term lysimeter case study by Meissner et al. (2007) and a long term investigation with a
68 surface energy budget model calibrated with micro-lysimeters by Jacobs et al. (2006) show that
69 rime, fog and dew contribute up to 5 % to the annual precipitation at a humid grassland site, and
70 are usually not captured by a standard precipitation gauge.

71 The eddy covariance (EC) method is one of the most established techniques to determine the
72 exchange of water, energy and trace gases between the land surface and the atmosphere. On the
73 basis of the covariance between vertical wind speed and water vapor density, the EC method
74 calculates the vertical moisture flux (and therefore ET) in high spatial and temporal resolution
75 with relatively low operational costs. The size and shape of the measurement area (EC footprint)
76 varies strongly with time (Finnigan, 2004). Under conditions of limited mechanical and thermal
77 turbulence the EC method tends to underestimate fluxes (Wilson et al., 2001; Li et al., 2008).
78 Energy balance deficits are on average found to be between 20 and 25% (Wilson et al., 2001;
79 Hendricks Franssen et al., 2010) and therefore latent heat flux or actual evapotranspiration
80 estimated from EC data shows potentially a strong underestimation. The energy balance closure
81 problem can be corrected by closure procedures using the Bowen ratio. However, this is
82 controversially discussed, especially because not only the underestimation of the land surface
83 fluxes, but also other factors like the underestimation of energy storage in the canopy might play
84 a role (Twine et al., 2000; Foken et al., 2011).

85 As an alternative to classical rain gauges and the eddy covariance method, state-of-the-art high
86 precision weighing lysimeters are able to capture the fluxes at the interface of soil, vegetation and
87 atmosphere (Unold and Fank, 2008). A high weighing accuracy and a controlled lower boundary
88 condition permit high temporal resolution precipitation measurements at ground level, including
89 dew, fog, rime, and snow. Additionally, ET_a can be estimated with the help of the lysimeter water
90 balance. However, the high acquisition and operational costs are a disadvantage of lysimeters.
91 Moreover, the accuracy of lysimeter measurements is affected by several error sources.
92 Differences in the thermal, wind and radiation regime between a lysimeter device and its
93 surroundings (oasis effect) (Zenker, 2003) as well as lysimeter management (e.g., inaccuracies in
94 biomass determination) can affect the measurements. Wind or animal induced mechanical
95 vibrations can influence the weighing system, but can be handled by accurate data processing
96 using filtering and smoothing algorithms (Schrader et al., 2013; Peters et al., 2014). Vaughan and
97 Ayars (2009) examined lysimeter measurement noise for data at a temporal resolution of one
98 minute, caused by wind loading. They presented noise reduction techniques that rely on Savitzky-
99 Golay (Savitzky and Golay, 1964) smoothing. Schrader et al. (2013) evaluated the different filter
100 and smoothing strategies for lysimeter data processing on the basis of synthetic and real
101 measurement data. They pointed out that the adequate filter method for lysimeter measurements

102 is still a challenge, especially at high temporal resolution, due the fact that noise of lysimeter
103 measurements varies strongly with weather conditions and mass balance dynamics.
104 Peters et al. (2014) recently introduced a filter algorithm for high precision lysimeters, which
105 combines a variable smoothing time window with a noise dependent threshold filter that accounts
106 for the factors mentioned above. They showed that their “Adaptive Window
107 and Adaptive Threshold Filter” (AWAT) improves actual evapotranspiration and precipitation
108 estimates from noisy lysimeter measurements compared to smoothing methods for lysimeter data
109 using the Savitzky-Golay filter or simple moving averages used in other lysimeter studies (e.g.,
110 Vaughan and Ayars, 2009; Huang et al., 2012; Nolz et al., 2013; Schrader et al., 2013).

111 In this work, a long term investigation to precipitation estimation with a lysimeter is presented.
112 One of the points of attention in the study is the contribution of dew and rime to the total
113 precipitation amount. The novelty compared to the work by Meissner et al. (2007) is the length of
114 the study and the fact that a series of six lysimeters is used. Our work allows corroborating results
115 from Jacobs et al. (2006), which used in their long term study a different, more uncertain
116 measurement method.

117 In the literature we find several comparisons between lysimeter measurements and standard ET
118 calculations. López-Urrea et al. (2006) found a good agreement of FAO-56 Penman-Monteith
119 with lysimeter data on an hourly basis. Vaughan et al. (2007) also reported a good accordance of
120 hourly lysimeter measurements with a Penman-Monteith approach of the California Irrigation
121 Management Information System. Wegehenkel and Gerke (2013) compared lysimeter ET with
122 reference ET and ET estimated by a numerical plant growth model. They found that lysimeter ET
123 overestimated actual ET, the cause being an oasis effect. On the other hand, also ET estimated by
124 EC measurements and water budget calculations are compared in literature. Scott (2010) found
125 that the EC-method underestimated evapotranspiration for a grassland site related to the energy
126 balance deficit. However, only a few comparisons between ET estimated by EC and lysimeter
127 data were found in literature. Chavez et al. (2009) evaluated actual evapotranspiration determined
128 by lysimeters and EC in the growing season for a cotton field site. They found a good agreement
129 of both methods after correcting the energy balance deficit and they suggested to consider also
130 the footprint area for EC calculations. Ding et al. (2010) found a lack of energy balance closure
131 and underestimation of ET_a by the EC-method for maize fields. An energy balance closure based
132 on the Bowen-Ratio method was able to reduce the ET-underestimation. Alfieri et al. (2012)

133 provided two possible explanations for a strong underestimation of EC-ET_a compared to
134 lysimeter ET_a. First, the energy balance deficit of the EC data, especially for those cases where
135 EC-measurements are affected by strong advection. Second, deviations between the vegetation
136 status of the lysimeter and the surrounding field. Evett et al. (2012) found an 18 %
137 underestimation of corrected EC-ET_a compared to ET_a estimated by lysimeter and attributed the
138 difference to differences in vegetation growth. Whereas above mentioned studies conclude that
139 deviations between ET_a measurements are related to vegetation differences, the EC footprint and
140 the ability to close the energy balance gap, the uncertainties of lysimeter measurements in this
141 context are hardly investigated. Lysimeter ET_a estimations often rely on relatively low temporal
142 resolution due to challenges in noise reduction, which impedes a simultaneous estimation of both
143 *P* and ET_a, by lysimeters. Furthermore, studies with cost and maintenance intensive lysimeters
144 are either with a few or without redundant devices, so that measurement uncertainty cannot be
145 addressed well.

146 The Terrestrial Environmental Observatories (TERENO) offer the possibility of detailed long-
147 term investigations of the water cycle components at a high spatio-temporal resolution (Zacharias
148 et al., 2011). This study compares precipitation and evapotranspiration estimates calculated with
149 a set of six weighing lysimeters (LYS) with nearby eddy covariance and precipitation
150 measurements for the TERENO grassland site Rollesbroich. Additional soil moisture, soil
151 temperature and meteorological measurements at this TERENO test site enable a detailed
152 analysis of differences between the different measurement techniques. The lysimeter data (ET_a-
153 LYS) are processed with the AWAT filter (Peters et al., 2014), which allows a simultaneous
154 estimation of *P* and ET_a in a high temporal resolution and the comparison is carried out with
155 energy balance corrected EC data (ET_a-EC). Actual ET estimates are additionally compared to
156 the full-form Penman-Monteith equation (Allen et al., 1998) accounting for the effects of variable
157 grass cover height. Precipitation measurements by a classical Hellmann type tipping bucket, with
158 and without accounting for wind and evaporation induced loss (Richter correction) were
159 compared with lysimeter data for one year (2012).

160 For our study, we (1) compared precipitation measurements by lysimeters and a (unshielded)
161 standard tipping bucket device and interpreted the differences. For example, the vegetated high
162 precision lysimeters potentially allow better estimates of precipitation accounting for dew, rime
163 and fog; (2) compared eddy covariance and lysimeter ET estimates and tried to explain

164 differences in estimated values; (3) tested whether a correction of the energy balance deficit for
165 the EC-method results in an ET_a estimate which is close to the lysimeter method; (4) analysed the
166 variability of the measurements by the six lysimeters under typical field conditions with identical
167 configuration and management.

168 **2. Material and Methods**

169 **2.1 Study Site and Measurement Setup**

170 The Rollesbroich study site (50° 37' 27" N, 6° 18' 17" E) is located in the TERENO Eifel low
171 mountains range/Lower Rhine Valley Observatory (Germany). This sub-catchment of the river
172 Rur has an area of 31 ha with an altitude ranging from 474 m to 518 m a.s.l.. The vegetation of
173 the extensively managed grassland site is dominated by ryegrass and smooth meadow grass. The
174 annual mean precipitation is 1033 mm and the annual mean temperature 7.7 °C (period 1981-
175 2001); these data are obtained from a meteorological station operated by the North Rhine-
176 Westphalian State Environment Agency (LUA NRW) at a distance of 4 km from the study site.
177 Fig. 1 shows a map of the study site and gives an overview of the installed measurement devices.

178 In 2010 a set of six lysimeters (TERENO-SoilCan project, UMS GmbH, Munich, Germany) was
179 arranged in a hexagonal design around the centrally placed service unit, which hosts the
180 measurement equipment and data recording devices. Each lysimeter contains silty-clay soil
181 profiles from the Rollesbroich site and is covered with grass. The conditions at the lysimeters
182 therefore closely resemble the ones in the direct surroundings (Fig. 2). Additionally, the spatial
183 gap between lysimeter and surrounding soil was minimized to prevent thermal regimes which
184 differ between the lysimeter and the surrounding field (oasis effect). Every lysimeter device has a
185 surface of 1 m², a depth of 1.5 m and is equipped with a 50 l weighted leachate tank connected
186 via a bidirectional pump to a suction rake in the bottom of each lysimeter. To reproduce the field
187 soil water regime, the lower boundary conditions are controlled by tensiometers (TS1, UMS
188 GmbH, Munich, Germany) monitoring the soil matric potential inside the lysimeter bottom and
189 the surrounding field. Matric potential differences between field and lysimeter are compensated
190 by suction rakes (SIC 40, UMS GmbH, Munich, Germany) injecting leachate tank water into the
191 lysimeter monolith during capillary rise or removing water during drainage conditions. The
192 weighing precision is 100 g for the soil monolith and 10 g for the leachate tank accounting for
193 long-term temperature variations and load alternation hysteresis effects. For short term signal
194 processing the relative accuracy for accumulated mass changes of soil monolith and leachate is
195 10 g. For the year 2012 measurements were made each 5 s and averaged to get minute values. In
196 the winter season a connection between the snow lying on the lysimeter and the surrounding
197 snow layer potentially disturbs the weighing system. A mechanical vibration plate is engaged at

198 all lysimeter devices to prevent this situation, and is activated once in 5 s between two
199 measurements. The lysimeters are also equipped with soil moisture, matric potential and
200 temperature sensors at different depths (10, 30, 50 and 140 cm). Amongst others, soil temperature
201 is determined in 10, 30 and 50 cm depth with PT-100 sensors integrated in TS1-tensiometers
202 (UMS GmbH, Munich, Germany). A schematic overview of the lysimeter device (Fig. 3) shows
203 the installation locations and the different sensor types. The lysimeter site was kept under video
204 surveillance by a camera taking a photo of the lysimeter status every hour. Further technical
205 specifications can be found in Unold and Fank (2008).

206 Latent and sensible heat fluxes were measured by an eddy covariance station at a distance of
207 approximately 30 m from the lysimeters. The EC-station (50° 37' 19" N, 6° 18' 15" E,
208 514 m a.s.l.) is equipped with a sonic anemometer (CSAT3, Campbell Scientific, Inc., Logan,
209 USA) at 2.6 m height to measure wind components. The open path device of the gas analyzer
210 (LI7500, LI-COR Inc., Lincoln, NE, USA) is mounted along with the anemometer at 2.6 m above
211 the ground surface and measures H₂O content of the air. Air pressure is measured at the
212 processing unit of the gas analyzer in a height of 0.57 m. Air humidity and temperature were
213 measured by HMP45C, Vaisala Inc., Helsinki, Finland (at 2.58 m above the ground surface).
214 Radiation was determined by a four-component net radiometer (NR01, Hukseflux Thermal
215 Sensors, Delft, Netherlands). Soil heat flux was determined at 0.08 m depth by a pair of two
216 HFP01 (Hukseflux Thermal Sensors, Delft, Netherlands).

217 Precipitation measurements are made by a standard Hellmann type tipping bucket balance (TB)
218 rain gauge (ecoTech GmbH, Bonn, Germany) with a resolution of 0.1 mm and a measurement
219 interval of 10 minutes. The measurement altitude of 1 m above ground is in accordance with
220 recommendations of the German weather service (DWD, 1993) for areas with an elevation
221 > 500 m a.s.l. and occasional heavy snowfall (WMO standard is 0.5 m). The unshielded gauge
222 was temporary heated during winter time to avoid freezing of the instrument.

223 Additional soil moisture and soil temperature measurements were carried out with a wireless
224 sensor network (SoilNet) installed at the study site (Qu et al., 2013). The 179 sensor locations at
225 the Rollesbroich site contain six SPADE sensors (model 3.04, sceme.de GmbH i.G., Horn-Bad
226 Meinberg, Germany) with two redundant sensors at 5, 20 and 50 cm depth. Further technical

227 details can be found in Qu et al. (2013). Soil water content and temperature were also measured
228 by two sensor devices installed nearby the lysimeter site.

229 2.2 Data Processing

230 2.2.1 Lysimeter

231 The lysimeter weighing data were processed in three steps:

232 1. Elimination of outliers by an automated threshold filter

233 2. Smoothing of measurement signal with the AWAT filter routine on the basis of data at a
234 temporal resolution of one minute

235 3. Estimation of hourly precipitation and evapotranspiration on the basis of the smoothed signal

236 Outliers were removed from the data by limiting the maximum weight difference between two
237 succeeding measurements for the soil column to 5 kg and for the leachate weight to 0.1 kg. The
238 lysimeter readings are affected by large random fluctuations caused by wind and other factors
239 that influence the measurement. Therefore, the AWAT filter (Peters et al., 2014) in a second
240 correction step was applied on the minute-wise summed leachate and on the weights for each
241 individual lysimeter. First, the AWAT routine gathers information about signal strength and data
242 noise by fitting a polynomial to each data point within an interval of 31 minutes. The optimal
243 order (k) of the polynomial is determined by testing different polynomial orders for the given
244 interval (i.e. k : 1-6) and selecting the optimal k according Akaike's information criterion (Akaike,
245 1974, Hurvich and Tsai, 1989). The maximum order of k is limited to six for the AWAT filter
246 preventing an erroneous fit caused by outliers. The average residual $s_{\text{res},i}$ of measured and
247 predicted values (Eq. 1) and the standard deviation of measured values $s_{\text{dat},i}$ (Eq. 2) lead to the
248 quotient B_i , which gives information about the explained variance of the fit and is related to the
249 coefficient of determination (R^2):

$$s_{\text{res},i} = \sqrt{\frac{1}{r} \sum_{j=1}^r [y_j - \hat{y}_j]^2} \quad (1)$$

$$s_{\text{dat},i} = \sqrt{\frac{1}{r} \sum_{j=1}^r [y_j - \bar{y}]^2} \quad (2)$$

$$B_i = \frac{s_{\text{res},i}}{s_{\text{dat},i}} = \sqrt{1 - R_i^2} \quad (3)$$

250 where y_j [M] is the measured data, \hat{y}_j [M] the fitted value at each time interval j , \bar{y} [M] the mean
 251 of the measurements and r the number of measurements within the given interval of data point i .
 252 $B_i = 0$ indicates that the polynomial totally reproduces the range of data variation in contrast to
 253 $B_i = 1$ where nothing of the variation in the data is explained by the fitted polynomial. Second,
 254 AWAT smoothes the data using a moving average for an adaptive window width w_i [T], which is
 255 a time dependent linear function of B_i (Eq. 4):

$$w_i(B_i) = \max(w_{\text{min}}, B_i w_{\text{max}}) \quad (4)$$

256
 257 where w_{max} [T] and w_{min} [T] are maximum and minimum provided window width. For our
 258 study w_{min} was set to 11 min, w_{max} was 61 min. A low B_i requires less smoothing and therefore
 259 small time windows, whereas a B_i close to one requires a smoothing interval close to the
 260 allowed w_{max} . Third, AWAT applies an adaptive threshold δ_i (Eq. 5) to the data at each time step
 261 to distinguish between noise and signal related to the dynamics of mechanical disturbances:

$$\delta_i = s_{\text{res},i} \cdot t_{97.5,r} \quad \text{for } \delta_{\text{min}} < s_{\text{res},i} \cdot t_{97.5,r} < \delta_{\text{max}} \quad (5)$$

262 where δ_i [M] is a function of the interval residuals ($s_{\text{res},i}$) [M] (see Eq. 1) and the Student t value
 263 ($t_{97.5,r}$) for the 95 % confidence level at each time step, δ_{min} [M] is the minimum and δ_{max} [M]
 264 is the maximum provided threshold for the mass change. The product of Student t and $s_{\text{res},i}$ is a
 265 measure for the significance level of mass changes during flux calculation. Hence, the δ_i value
 266 indicates the range ($\pm s_{\text{res},i} \cdot t_{97.5,r}$), where the interval data points differ not significantly from
 267 the fitted polynomial at the 95 % confidence level. Mass changes above the adaptive threshold
 268 δ_i are significant and interpreted as signal, whereas weight differences below δ_i are interpreted as
 269 noise. The adaptive threshold is limited by δ_{min} and δ_{max} to guarantee that (1) mass changes
 270 smaller than the lysimeter measurement accuracy are understood as remaining noise and
 271 therefore not considered for the flux calculation and (2) noise is not interpreted as signal during
 272 weather conditions, which produce noisy lysimeter readings (i.e. thunderstorms with strong wind
 273 gusts). Lysimeter calibration tests with standard weights at the study site indicate a system scale
 274 resolution of 0.05 kg. We chose a slightly higher threshold ($\delta_{\text{min}} = 0.055$ kg) with an adequate

275 tolerance for our TERENO lysimeter devices. For the upper threshold $\delta_{\max} = 0.24$ kg was taken,
276 similar to the example presented by Peters et al. (2014).

277 For the separation of precipitation and actual evapotranspiration (ET_a) AWAT assumes that
278 increases of lysimeter and leachate weights (averaged over a period of one minute) are
279 exclusively related to precipitation and negative differences to ET_a [$M T^{-1}$]. Supposing that no
280 evapotranspiration occurs during a precipitation event and assuming a fixed water density of
281 1000 kg m^{-3} , precipitation (P) [$M T^{-1}$] can be derived from the lysimeter water balance (Eq. 7)
282 as:

$$ET_a = P - L - \frac{dS_S}{dt} \quad (6)$$

$$P = L + \frac{dS_S}{dt} \quad (7)$$

283
284 where L is the amount of leachate water [$M T^{-1}$] and dS_S/dt is the change of soil water storage
285 [$M T^{-1}$] with time. After smoothing the fluxes at one minute resolution were cumulated to hourly
286 sums of P and ET_a .

287 Although the six lysimeters have a similar soil profile, technical configuration and management
288 (i.e. grass cut, maintenance), differences in measured values between lysimeters are not
289 exclusively related to random errors. Systematic weight variations may for example be caused by
290 soil heterogeneity, mice infestation and differences in plant dynamics. In this study precipitation
291 measured by lysimeter and TB are compared, as well as evapotranspiration measured by
292 lysimeter and eddy covariance. The precipitation or ET_a averaged over the six redundant
293 lysimeters are used in this comparison. We assume that the lysimeter average of six redundant
294 lysimeter devices is the most representative estimation for the lysimeter precipitation and actual
295 evapotranspiration (unless specified otherwise).

296 2.2.2 Eddy Covariance Data

297 Eddy covariance raw measurements were taken with a frequency of 20 Hz and fluxes of sensible
298 heat (H) and latent heat (LE) were subsequently calculated for intervals of 30 minutes by using
299 the TK3.1 software package (Mauder and Foken, 2011). The complete post-processing was in
300 line with the standardized strategy for EC data calculation and quality assurance presented by
301 Mauder et al. (2013). It includes the application of site specific plausibility limits and a spike
302 removal algorithm based on median absolute deviation of raw measurements, a time lag
303 correction for vertical wind speed with temperature and water vapor concentration based on
304 maximizing cross-correlations between the measurements of the used sensors, a planar fit
305 coordinate rotation (Wilczak et al., 2001), corrections for high frequency spectral losses (Moore
306 1986), the conversion of sonic temperature to air temperature (Schotanus et al., 1983) and the
307 correction for density fluctuations (Webb et al., 1980). Processed half hourly fluxes and statistics
308 were applied to a three-class quality flagging scheme, based on stationarity and integral
309 turbulence tests (Foken and Wichura, 1996) and classified as high, moderate and low quality
310 data. For this analysis only high and moderate quality data were used, while low quality data
311 were treated as missing values. To assign half hourly fluxes with its source area the footprint
312 model of Korman and Meixner (2001) was applied.

313 Almost every eddy covariance site shows an unclosed energy balance, which means that the
314 available energy (net radiation minus ground heat flux) is found to be larger than the sum of the
315 turbulent fluxes (sensible plus latent heat flux) (Foken, 2008; Foken et al., 2011). In this study the
316 energy balance deficit (EBD) was determined using a 3-h moving window around the
317 measurements (Kessomkiat et al., 2013):

$$318 \quad \text{EBD}_{3h} = R_{n-3h} - (G_{3h} + \text{LE}_{3h} + H_{3h} + S_{3h}) \quad (8)$$

319
320 where R_{n-3h} is average net radiation [M T^{-3}], G_{3h} is average soil heat flux [M T^{-3}], LE_{3h} is
321 average latent heat flux [M T^{-3}], H_{3h} is average sensible heat flux [M T^{-3}], and S_{3h} is average heat
322 storage (canopy air space, biomass and upper soil layer above ground heat flux plate) [M T^{-3}]. All
323 these averages are obtained over a three hour period around a particular 30 min EC-measurement.
324 The moving window of three hours is a compromise between two sources of error. First, it
325 guarantees a relatively small impact of random sampling errors and therefore increases the

326 reliability of the EBD calculation. Second, the relatively short interval ensures that the
 327 calculations are not too much affected by non-stationary conditions. It was assumed that the
 328 energy balance deficit is caused by an underestimation of the turbulent fluxes and therefore the
 329 turbulent fluxes are corrected according to the evaporative fraction. The evaporative fraction (EF)
 330 was determined for a time window of seven days:

$$331 \quad EF = \frac{\overline{LE}_{7d}}{\overline{LE}_{7d} + \overline{H}_{7d}} \quad (9)$$

332
 333 where \overline{LE}_{7d} and \overline{H}_{7d} [$M T^{-3}$] are the latent and sensible heat fluxes averaged over seven days. The
 334 chosen time period increases the reliability for EF calculation compared to single days. Dark days
 335 with small fluxes may not give meaningful results. Kessomkiat et al. (2013) investigated the
 336 impact of the time window on the calculation of the EF and found that a moving average over
 337 seven days gives good results, whereas a too short time window of one day gives unstable,
 338 unreliable results.

339 The energy balance corrected latent heat flux was determined by redistribution of the latent heat
 340 on the basis of the calculated evaporative fraction:

$$341 \quad LE_{0.5h}^* = LE_{0.5h} + EBD_{3h}(EF) \quad (10)$$

342
 343 where $LE_{0.5h}^*$ is the latent heat flux (for a certain measurement point in time; i.e. a 30 minutes
 344 period for our EC data). The EBD is added to the uncorrected LE according to the partitioning of
 345 heat fluxes in the EF. Further details on the EBD correction method can be found in Kessomkiat
 346 et al. (2013).

347 In this study, also the evapotranspiration (ET_a -EC) calculated with the original latent heat flux
 348 (not corrected for energy balance closure) will be presented for comparison. Furthermore, the
 349 most extreme case would be that the complete EBD is linked to an underestimation of the latent
 350 heat flux. Some authors argue (Ingwersen et al., 2011) that the EBD could be more related to
 351 underestimation of one of the two turbulent fluxes than the other turbulent flux. Therefore, as an
 352 extreme scenario the complete EBD is assigned to underestimation of the latent heat flux.

353

354 ET_a -EC is calculated from the latent heat flux according to:

355
$$ET_a = \frac{LE_h^*}{L(T_h)_{H_2O} * \rho_{H_2O}} \quad (11)$$

356

357 where ET_a is ET_a -EC [$L T^{-1}$], LE_h^* is latent heat flux [$M T^{-3}$], ρ is the density of water [$M L^{-3}$] and
358 $L(T_h)_{H_2O}$ is the vaporization energy [$L^2 T^{-2}$] at a given temperature.

359 The lysimeters are thought to be representative for the EC footprint, although size and shape of
360 the EC footprint are strongly temporally variable. However, the EC footprint is almost
361 exclusively constrained to the grassland and the lysimeters are also covered by grass.

362 2.2.3 Grass Reference Evapotranspiration

363 The measurements of ET_a by the EC-method and lysimeters were in this study compared with
 364 evapotranspiration calculated with full-form Penman-Monteith equation as presented by Allen et
 365 al. (1998). This approach accounts for vegetation and ground cover conditions during crop stage
 366 considering bulk surface and aerodynamic resistances for water vapor flow. The calculations
 367 were adapted for hourly intervals according to Eq. 12:

$$368 \quad ET_{PM} = \frac{0.408\Delta(R_n - G) + \gamma \frac{3600\varepsilon}{T_{vh}R(r_a u_2)} u_2 (e^\circ(T_h) - e_a)}{\Delta + \gamma(1 + \frac{r_s}{r_a})} \quad (12)$$

371 where ET_{PM} is the hourly Penman-Monteith evapotranspiration [$L T^{-1}$], R_n is net radiation at the
 372 grass surface [$M T^{-3}$], G is soil heat flux density [$M T^{-3}$], T_{vh} is mean hourly virtual temperature
 373 [θ], R is the specific gas constant for dry air [$L^2 T^{-2} \theta^{-1}$], r_a is the aerodynamic resistance [$T L^{-1}$],
 374 r_s is the (bulk) surface resistance [$T L^{-1}$], ε is the ratio molecular weight of water vapour (dry air)
 375 [-], T_h is mean hourly air temperature (θ), Δ slope of the saturated vapour pressure curve at T_h
 376 [$M L^{-1} T^{-2} \theta^{-1}$], γ is psychrometric constant [$M L^{-1} T^{-2} \theta^{-1}$], $e^\circ(T_h)$ is saturation vapour pressure
 377 for the given air temperature [$M L^{-1} T^{-2}$], e_a is average hourly actual vapour pressure [$M L^{-1} T^{-2}$],
 378 and u_2 is average hourly wind speed [$L T^{-1}$] at 2 m height. All required meteorological input
 379 parameters for calculating ET_{PM} were taken from the EC station. The wind speed data were
 380 corrected to 2 m using the FAO-standard wind profile relationship of Allen et al. (1998).

381 We approximated aerodynamic resistance (r_a), (bulk) surface resistance (r_s) and leaf area index (LAI)
 382 with help of grass height according to Allen et al. (2006):

$$r_a = \frac{\ln \left[\frac{z_m - \frac{2}{3} h_{plant}}{0.123 h_{plant}} \right] \ln \left[\frac{z_h - \frac{2}{3} h_{plant}}{0.1 (0.123 h_{plant})} \right]}{k^2 u_2} \quad (13)$$

383

384

$$r_s = \frac{r_i}{\text{LAI}_{\text{act}}} \quad (14)$$

385

$$\text{LAI}_{\text{act}} = (0.3 \text{ LAI}) + 1.2 = 0.5 (24 h_{\text{plant}}) \quad (15)$$

386

387 where z_m is the height of the wind measurement [L], z_h is the height of the humidity
388 measurement [L], h_{plant} is the grass length [L] at the lysimeter, k is the von Karman's constant
389 [-], r_i the stomatal resistance [T L^{-1}], and LAI_{act} the active leaf area index taking into account that
390 only the upper grass surface contributes to heat and vapor transfer [-]. For our calculations we
391 assume a fixed stomatal resistance for a well-watered grass cover of 100 s m^{-1} in accordance to
392 Allen et al. (1998). The grass length at the lysimeters was estimated with the help of maintenance
393 protocols and the surveillance system. Grass lengths between two measurement intervals were
394 linearly interpolated on a daily basis.

395 2.2.4 Precipitation Correction

396 A precipitation correction according the method of Richter (1995) was applied (Eq. 16, 17) on a
397 daily basis to account for wind, evaporation and wetting losses of the tipping bucket
398 precipitation:

$$399 \quad P^{cor} = P + \Delta P \quad (16)$$

$$400 \quad \Delta P = bP^\epsilon \quad (17)$$

401 where P^{cor} is the corrected daily precipitation [$M T^{-1}$], P is the measured tipping bucket
402 precipitation [$M T^{-1}$], ΔP the estimated precipitation deficit [$M T^{-1}$], b the site specific wind
403 exposition coefficient [-], and ϵ the empiric precipitation type coefficient [-].

404 This correction method is widely used for German weather service stations and relies on empirical
405 relationships of precipitation type and wind exposition, without using direct wind measurements. In
406 order to determine both empirical coefficients, we categorized the precipitation type with the help
407 of air temperatures on a daily basis. It was assumed that temperatures below 0 °C result in solid
408 precipitation, temperatures between 0 °C and 4 °C give mixed precipitation and air temperatures
409 above 4 °C only liquid precipitation. Furthermore, the rain gauge is located in an open area and
410 the summer period was defined from May to September and the winter period from October to
411 April. The corresponding correction coefficients were calculated according to Richter (1995) and
412 are provided in Tab. 1.

413 3. Results and Discussion

414 3.1 Precipitation Measurements

415 Tab. 2 shows the monthly precipitation sums measured by the tipping bucket (TB) and calculated
416 from the lysimeter balance data for the year 2012. The precipitation difference between both
417 devices for the year 2012 is 145.0 mm implying a 16.4 % larger average lysimeter precipitation
418 than TB. For the individual lysimeters the yearly precipitation ranges from 996.2 mm to
419 1037.7 mm (-3.0 to +1.0 % compared to the lysimeter average). This implies that the minimum
420 and maximum precipitation differences between individual lysimeters and TB were 114.1 mm
421 (12.9 %) resp. 155.6 mm (17.6 %), where precipitation for lysimeters was always higher than for
422 TB. The monthly precipitation sums for the period April-October measured by the tipping bucket
423 are smaller than the ones from the lysimeter average and differences range between 1 % in July
424 and 42 % in September. The winter months show higher relative differences. The highest
425 difference was found in March 2012, when the lysimeters registered an amount of precipitation
426 double as large as the TB. The precipitation sums measured by lysimeter and tipping bucket
427 correlate well on an hourly basis, especially from April to October with R^2 varying between 0.74
428 (Apr) and 0.99 (May), but with the exception of September (0.58). For winter months the
429 explained variance is smaller with a minimum of 13% for February 2012.

430 The period April – August shows the smallest precipitation differences among the six lysimeters
431 with monthly values of ± 5 % in relation to the lysimeter average. In contrast, February,
432 September, and December exhibit the highest absolute and relative precipitation differences
433 among lysimeters with variations between -13 and 13 mm (± 35 %) with respect to the mean.
434 Fig. 4 shows the absolute daily differences in precipitation between lysimeter and TB
435 measurements. It shows that the cases where lysimeters register slightly higher monthly
436 precipitation sums than TB are related to single heavy rainfall events (June, July). In contrast,
437 especially for February, the beginning of March, and the first half of December, larger
438 fluctuations in differences between daily precipitation measured by TB and lysimeter are found,
439 with less precipitation for TB than for lysimeters most of the days. These periods coincide with
440 freezing conditions and frequent episodes with sleet or snowfall. According to Nešpor and
441 Sevruk (1999) these weather conditions are typically associated with a large tipping bucket
442 undercatch because snowflakes are easier transported with the deformed wind field around a rain

443 gauge. The surveillance system, which is installed at the lysimeter site, gives support for these
444 findings. For example, a sleet precipitation event on March 7th explains 70 % (8.5 mm) of the
445 monthly precipitation difference between lysimeter and TB. At this day the wind speed during the
446 precipitation event was relatively high (4.4 m s^{-1}) and precipitation intensity varied between 0.6
447 and 2.9 mm h^{-1} . In general, winter measurement inaccuracies can be caused by frozen sensors and
448 snow or ice deposit on the lysimeter surface. This situation may cause ponding effects close to
449 the soil surface in the lysimeter and superficial runoff. In order to further address the lysimeter
450 uncertainty, we calculated the average cumulative drainage and soil water storage with minimum
451 and maximum ranges for the individual lysimeters (Fig. 5). The soil water storage was
452 determined by the remaining term of the water balance on a daily basis. The total drainage,
453 averaged over the six lysimeters was 411.2 mm for 2012 with a variation between 385.5 and
454 440.4 mm. The soil moisture storage change over the year varies between -5.1 mm to 28.3 mm
455 with an average of +11.2 mm. The assessment of drainage volumes and changes in soil water
456 storage was somewhat hampered by erroneous data related to drainage leakage (January) or
457 system wide shut down due to freezing. However, the uncertainty in the water balance during
458 those periods should have a minor effect on the short term calculations of lysimeter P and ET_a .

459 In order to explain differences in precipitation amounts between lysimeter and tipping bucket, the
460 contribution of dew and rime to the total yearly precipitation amount was determined. The hourly
461 data of lysimeter and TB were filtered according meteorological criteria. First, meteorological
462 conditions were selected which favor the formation of dew, rime, fog and mist. Selected were
463 small precipitation events between sunset and sunrise associated with high relative humidity ($>$
464 90%), negative net radiation and low wind speed ($< 3.5 \text{ m s}^{-1}$). Under these meteorological
465 conditions it is probable that dew or rime is formed after sunset and before sunrise on cloud free
466 days. For these days the difference in precipitation between TB and lysimeter is calculated if TB
467 shows no precipitation signal or if the lysimeter has no precipitation signal. For the first case
468 ($P-TB=0$) the total amount of the lysimeter precipitation is 24.5 mm, which contributes 16.9 % to
469 the total yearly precipitation difference with the TB (and 2.4% of the yearly lysimeter
470 precipitation). The period from April to August shows in general smaller precipitation amounts
471 related to such situations. In contrast, likely dew and rime conditions where lysimeter
472 precipitation is zero have a registered amount of TB-precipitation of 1.7 mm, which is only 0.2 %
473 of the total measured TB amount for the considered period. A closer inspection of the

474 precipitation data shows that both devices are able to capture dew and rime. However, a delay of
475 some hours between TB and lysimeters was found. It is supposed that dew or fog precipitation
476 was cumulating in the TB device until the resolution threshold of 0.1 mm was exceeded. This
477 indicates that the TB resolution of 0.1 mm is too coarse to detect small dew and rime amounts in
478 a proper temporal assignment. This confirms the expected ability of the lysimeter to measure
479 rime and dew better than Hellman type pluviometers or tipping bucket devices. The surveillance
480 system was used to check whether indeed dew/rime was formed on the before-mentioned days.
481 On days which fulfilled the criteria and air temperatures close to or below 0 °C rime was seen on
482 the photos. For days that fulfilled the conditions and temperatures above 0 °C camera lenses were
483 often covered with small droplets.

484 Weather conditions with drizzle or fog occur frequently at the study site. This is related to humid
485 air masses from the Atlantic which are transported with the dominating Southwestern winds and
486 lifted against the hills in this region. The surveillance system was used to detect fog and drizzle
487 situations during the year 2012. For those situations, a difference in precipitation between TB and
488 lysimeters of 8 mm was found, which contributes 5.5 % to the yearly difference of both devices.
489 Fig. 6 illustrates the example of May 5 – May 6 2012. The hourly photos of the site show drizzle,
490 light rain and fog for this period. For both days the air temperature is close to the dew point
491 temperature. The precipitation difference between tipping bucket and lysimeter over this period
492 was 4.0 mm (Σ TB: 12.8 mm, Σ LYS: 16.8). The maximum difference was 0.5 mm and found at
493 6 h on the 5th of May in combination with fog. On May 5 during these conditions hourly TB
494 precipitation is often zero and LYS mean precipitation rates are small (0.02 - 0.2 mm hr⁻¹). The
495 comparison of individual lysimeter devices shows that not every lysimeter exceeds the predefined
496 lower threshold of 0.055 mm for the AWAT filter (i.e. 5th of May 15:00, 6th of May 01:00- 03:00
497 LT). However, in these cases at least three lysimeters show a weight increase, which supports the
498 assumption that a real signal was measured instead of noise.

499 With the purpose of explaining the remaining difference in precipitation amount between TB and
500 lysimeter, the relationship between wind speed and the precipitation differences was examined.
501 The determined precipitation differences could in theory be explained by undercatch related to
502 wind (Sevruk, 1981 & 1996). It was checked whether correcting the tipping bucket data (TB_{corr})
503 according to the method of Richter (1995) could reduce the precipitation difference between
504 lysimeter and TB. The total precipitation sum after correction is 996.9 mm for 2012, only 3%

505 smaller than the yearly lysimeter average and within the range of the individual lysimeters. The
506 correction of TB data in general decreased the differences in the winter period (January – March,
507 November - December). However, for the summer period the monthly precipitation sum of TB_{corr}
508 mainly overestimated precipitation and tended to slightly increase the precipitation differences.
509 In order to explore this relation further we examined the correlation between wind speed and
510 precipitation residuals and found almost no correlation (Fig. 7). A possible explanation is that
511 other potential dew or rime situations are not properly filtered by the used criteria (e.g, dew
512 occurs in case the net radiation is slightly positive or close to zero). Additionally, the correlation
513 between undercatch and wind speed is dependent on precipitation type, intensity and drop size,
514 for which information was limited during the investigation period. To investigate these relations
515 we used the classification of precipitation types as outlined before. The contribution of liquid
516 precipitation to total yearly precipitation is 80.9 % for the TB and 74.7 % for the lysimeters. The
517 relative amount of solid precipitation was also different between the two measurement methods.
518 Whereas for the lysimeters 7.8 % (79.7 mm) was classified as solid precipitation, the TB had only
519 0.6 % (5.6 mm) during periods with temperature < 0 °C. In relation to the total precipitation
520 difference of 145 mm this means that 51 % of the difference was associated with solid
521 precipitation events and 37 % with liquid precipitation events, which indicates the relatively large
522 contribution of solid precipitation events to the total difference. The transition range (0-4 °C)
523 makes up 12 % of the total difference. Moreover, it was found that 78.7 % of the solid
524 precipitation came along with small precipitation intensities (< 1.0 mm h⁻¹) and low wind speeds
525 (< 2.0 m s⁻¹). The surveillance system allowed to further investigate these large precipitation
526 differences for air temperatures below zero. The snow depth at the lysimeters and surrounding
527 areas is also an indication of precipitation amounts, assuming that 1 cm snow height corresponds
528 to 1 mm precipitation. This method revealed that for conditions of light to moderate snowfall (< 4
529 mm h⁻¹ precipitation intensity) the TB had a precipitation undercatch in January, February and
530 December of 11.4 mm (7.9 % of total precipitation difference). The registered precipitation
531 amount of the lysimeter under those conditions was realistic. However, during periods where the
532 lysimeters were completely covered by snow (e.g. 1 – 15 February) precipitation estimates by
533 lysimeter (up to 16 mm d⁻¹ difference with tipping bucket) could not be confirmed by the camera
534 system and were most probably influenced by snow drift or snow bridges. These situations
535 explain 35.8 % (51.9 mm) of the total precipitation difference for 2012. For solid precipitation
536 events a relationship (R²=0.5) between precipitation differences and wind speed was found, but

537 the number of datapoints was very limited (n=7). For conditions of liquid precipitation no
538 correlation was found between residuals and wind speed ($R^2 < 0.02$).

539

540 3.2 Comparison of Evapotranspiration

541 In general, the yearly sums of ET_{PM} and ET_a -LYS were slightly higher than ET_a -EC; 6.1 % for
542 ET_{PM} and 2.4 % for ET_a -LYS. The minimum ET_a of the individual lysimeter measurements (ET_a -
543 LYSmin) is 467.1 mm, which is 7.9 % smaller than the lysimeter average (507.4 mm); the
544 maximum (ET_a -LYSmax) is 523.1 mm (+ 3.1 %). This indicates that in general over the year
545 2012 evapotranspiration was limited by energy and not by water, as actual evapotranspiration
546 was close to a theoretical maximum value for well watered conditions as estimated by ET_{PM} . This
547 also implies that our assumption of a stomatal resistance corresponding to well-watered
548 conditions was justified. Water stress conditions would lead to decreased plant transpiration rates
549 and increased stomatal resistance. Tab. 3 lists the evapotranspiration results of January –
550 December 2012. In 2012 ET_{PM} was always close to ET_a -LYS and ET_a -EC and there are no
551 months that ET_{PM} is clearly larger than measured actual evapotranspiration by lysimeter and eddy
552 covariance. Root mean square errors of hourly ET_a sums vary between 0.01 mm h⁻¹ in winter and
553 0.11 mm h⁻¹ in summer months and are in phase with the seasonal ET dynamics.

554 We focus now on the comparison of monthly ET_a -LYS and ET_a -EC sums within the investigated
555 period. During winter periods with low air temperatures and snowfall ET_a -LYS and ET_a -EC
556 showed larger relative differences. For the period March to May ET_a -LYS and ET_a -EC differ
557 approx. 6 % and ET_a -LYS exceeds ET_a -EC from June to August by 12 %. The larger difference
558 in August (23 %) explains the yearly difference between ET_a -EC and ET_a -LYS. Hourly actual
559 evapotranspiration from lysimeter and hourly actual evapotranspiration from EC are strongly
560 correlated, but correlation is lower in the winter months. The registered monthly ET by the
561 different lysimeters shows the largest variations in July with amounts that are up to 14.0 mm
562 lower and 8.0 mm higher than the ET averaged over all six lysimeters.

563 Fig. 8 shows the cumulative curve of the daily ET_a -LYS and ET_a -EC compared to ET_{PM} for 2012.
564 From end of March 2012 the sums of ET_a -LYS and ET_a -EC tend to converge, but at the end of
565 May ET_a -EC exceeds ET_a -LYS. In June and July ET_a -LYS and ET_a -EC are very similar, but in
566 August ET_a -LYS is larger than ET_a -EC. After August the difference between ET_a -LYS and
567 ET_a -EC does not increase further. The area in grey represents the range of minimum and
568 maximum cumulative ET_a -LYS, measured by individual lysimeters. Until August ET_a -EC and
569 ET_{PM} are slightly higher or close to the maximum measured ET_a -LYS. In August ET_{PM} increases
570 further, whereas ET_a -EC falls below the minimum lysimeter value. Additionally, Fig. 8 shows the

571 course of the ET_a -EC without correction for EBD and for ET_a -EC max.. ET_a -uncorr is ca.
572 411 mm over this period, whereas ET_a -EC max is 567 mm, which shows the large potential
573 uncertainty of the EC-data. The comparison illustrates that the application of the Bowen ratio
574 correction to the EC data results in an actual evapotranspiration estimate close to the actual
575 evapotranspiration from the lysimeter, whereas ET_a -EC uncorr is much smaller than the lysimeter
576 evapotranspiration. Tab. 4 lists the monthly latent heat fluxes, the corrected LE fluxes (on the
577 basis of the Bowen ratio) and the mean differences between both. It was found that the absolute
578 difference is between 29.8 W m^{-2} (August 2012) and 3.2 W m^{-2} (February 2012). The EBD
579 ranges from 12.6 % - 24.2 % for the period April to September. The yearly maximum was found
580 in February with 36.9 %. EB deficits are site-specific, but these findings confirm the importance
581 of EC data correction as suggested by Chavez et al. (2009).

582 In order to explain the differences between ET_{PM} , ET_a -EC and ET_a -LYS, we investigated the
583 variations in radiation, vegetation and temperature regime and their impact on ET in more detail.
584 The albedo could be estimated according to the measured outgoing shortwave radiation at the
585 EC-station divided by the incoming shortwave radiation, also measured at the EC-station. The
586 yearly mean albedo is 0.228, which is close to the assumed albedo of 0.23 for grassland.
587 However, some periods (i.e. periods with snow cover) have a much higher albedo. Although
588 albedo variations between different vegetation growth stages at different fields at the study site
589 were considered as explanation for differences in ET_a , we assume similar albedo for ET_a -EC and
590 ET_a -LYS measurement due to the central location of of the radiation measurements between the
591 relevant fields.

592 The grass length is related to the LAI, which impacts water vapor flow at the leaf surface. Under
593 well-watered conditions more surface for plant transpiration leads in general to higher
594 transpiration rates by decreasing the bulk surface resistance. Fig. 9 shows that the grass length
595 measured at the Rollesbroich site is up to 80 cm before cutting. Unfortunately, grass height
596 measurements are not available for the lysimeters but only for the surrounding field. It is
597 assumed, on the basis of information from the video surveillance system, that grass heights
598 generally are in good agreement between lysimeters (lysimeter site) and the surrounding field
599 (lysimeter field), which allows a reconstruction of the grass length illustrated in Fig. 9. However,
600 the grass harvesting dates of lysimeters and surrounding field deviate in August and September
601 and are given for the lysimeters in Fig. 9.

602 Fig. 10 illustrates the differences of the measured daily ET_a sums between lysimeter and EC.
603 High positive and negative differences up to 2.1 mm/day were found from March 2012 –
604 September 2012. In general, the differences of ET_a -LYS and ET_{PM} show smaller fluctuations than
605 the differences of ET_a -EC and ET_{PM} . It was found that lysimeter harvesting affects the
606 differences between ET_a -LYS and ET_{PM}/ET_a -EC. The differences were positive before harvesting
607 and negative after harvesting indicating ET_a reduction due to the grass cutting effects. For the
608 period from the 21st of May to the 3rd of July, a period with high grass length differences (Fig. 9)
609 between the lysimeter site and the field behind the EC-station, ET_a differences (ET_a -EC - ET_a -
610 LYS) and grass length differences show a good correlation ($R^2=0.58$), which is illustrated in Fig.
611 11. During the period with maximum grass length difference (24 May – 1 June) ET_a -EC is 26 %
612 higher than ET_a -LYS. The differences between ET_a -EC and ET_{PM} do not show such a significant
613 correlation with grass heights, although the relationship in August is in correspondence with the
614 differences of ET_a -EC and ET_a -LYS. This could be related to the EC-footprint, because the EC
615 station is centrally located in between the two investigated fields with different grass lengths. The
616 EC-footprint might also include other surrounding fields with different grass heights. 80 % of the
617 EC footprint is located within a radius of 100 m of the EC tower, and 70 % in a radius of 40 m,
618 which is the approximate lysimeter distance. Therefore, the ET_a -EC estimations represent a
619 spatial mean of a wider area, where cutting effects are averaged compared to the lysimeter point
620 measurements. Fig. 12 shows the mean hourly ET_a rates of lysimeter and EC as well as the ET_{PM}
621 for 2012. In general, the daily courses and the daily maxima of ET_a -LYS, ET_{PM} and ET_a -EC
622 correspond well. ET_a -EC shows higher peaks at noon in May and September compared to ET_a -
623 LYS, but corresponds well to ET_{PM} . In contrast, ET_a -LYS exhibits the highest rates from June to
624 August. The absence of a harvest of the lysimeter in August and the first September decade (in
625 contrast to the surrounding fields) leads to potentially increased lysimeter ET_a measurements as
626 compared to the surroundings due to an island position.

627 In order to examine whether lysimeter measurements could have been affected by a soil
628 temperature regime different from the field, the temperature regimes of the lysimeters were
629 compared to the field temperature. Fig. 13 shows the daily mean soil temperature differences
630 between the lysimeters, a nearby SoilNet device (SN 30) and the mean of all available SoilNet
631 devices installed at the southern study site. SoilNet temperatures were measured 5 cm below
632 surface; lysimeter temperature measurements were conducted with SIS sensors in 10 cm depth.

633 The temperature differences between the lysimeter and the nearby SoilNet device and the SoilNet
634 mean are less than 1 K, which is as well the range of variation of the SoilNet device with respect
635 to the SoilNet mean. In general the temperature differences increase until noon and then decrease
636 again. Positive differences from May to July indicate higher lysimeter soil temperatures than the
637 surroundings. However, a clear indicator for a bias caused by an oasis effect in the lysimeter
638 measurements was not found. Feldhake and Boyer (1986) describe the effect of soil temperature
639 on evapotranspiration for different grass types, which allow an estimation of ET_a increase caused
640 by a differing lysimeter temperature regime. They showed that daily ET_a rates can increase with
641 an increase of soil temperature (i.e. daily Bermuda grass ET_a rate increases from 4.3 mm/day to
642 6.4 mm/day (49 %) for a soil temperature increase from 13 to 29 °C). We used this linear
643 relationship to roughly estimate the effect on ET_a for the period May – August on a daily basis.
644 For this period the measured soil temperature with SN(30) for daylight hours ranged between
645 9.5 and 15.1 °C and between 9.3 and 15.5 °C for the lysimeter mean (SIS sensors). The mean
646 difference is 0.67 K. This results in a total ET_a increase of 8.8 mm or 2.5 % in relation to the total
647 ET_a -LYS of 349 mm on the basis of hourly ET. Therefore, the effect of increased soil
648 temperature in the lysimeter is most probably limited, but not negligible.

649 **4. Conclusions**

650 This study compares evapotranspiration and precipitation estimates calculated using a set of six
651 redundant weighable lysimeters with nearby eddy covariance and precipitation measurements at a
652 TERENO grass land site in the Eifel (Germany) for one year (2012). The lysimeter data at a
653 temporal resolution of one minute are processed with the AWAT filter (Peters et al., 2014),
654 which takes account of the lysimeter noise due to random fluctuations caused by changing
655 weather conditions. Additional precipitation measurements were conducted with a classical
656 unshielded Hellmann type tipping bucket and compared with lysimeter data. For the ET_a
657 comparison eddy covariance (EC) data is corrected for the energy balance deficit using the
658 Bowen ratio method. Additionally, evapotranspiration and the evapotranspiration according the
659 full-form Penman-Monteith equation were calculated.

660 The estimated hourly precipitation amounts derived by lysimeter and tipping bucket data show
661 significant differences and the total precipitation measured by the lysimeter is 16.4 % larger than
662 the tipping bucket amount. The relative differences in the monthly precipitation sums are small in
663 the summer period, whereas high differences are found during the winter season. The winter
664 months with solid precipitation exhibit the lowest correlations between lysimeter and tipping
665 bucket amounts. Precipitation was measured by six different lysimeters and yearly amounts for
666 individual lysimeters showed variations of -3.0 to 1.0 % compared to the yearly precipitation
667 mean over all lysimeters. An additional comparison with corrected tipping bucket precipitation
668 measurements according to the method of Richter (1995) shows in general a decrease of the
669 monthly and yearly difference, which was 3 % after correction. In order to explain the differences
670 in precipitation between the devices the contribution of dew, rime and fog to the yearly
671 precipitation was analyzed. This was done by filtering the data for typical weather conditions like
672 high relative humidity, low wind speed and negative net radiation which promote the
673 development of dew and rime. For the identified cases a check was made with a visual
674 surveillance system whether dew/rime was visible. During these conditions the lysimeter shows
675 clearly larger precipitation amounts than the TB, which explains 16.9 % of the yearly
676 precipitation difference. Fog and drizzling rain conditions, additionally identified with the help of
677 the on-site camera system, explain another 5.5 % of the yearly precipitation differences. These
678 findings indicate an improved ability of the lysimeters to measure dew and rime as well as fog
679 and drizzling rain. The remaining 78 % of the precipitation difference between lysimeters and

680 tipping bucket is strongly related to snowfall events, as under those conditions large differences
681 were found. Lysimeter precipitation measurements are affected by a relatively high measurement
682 uncertainty during winter weather conditions similar to TB and other common measurement
683 methods. Thus, the limitations for the lysimeter precipitation measurements during those periods
684 need further investigation. We found that during conditions where the lysimeters were completely
685 covered by snow, lysimeter records were unreliable, and contributed to 36 % of the total
686 precipitation difference.

687 Actual evapotranspiration measured by the eddy covariance method (ET_a -EC) and lysimeter
688 (ET_a -LYS) showed a good correspondence for 2012, with larger relative differences and low
689 correlations in winter in contrast to high correlations and smaller relative differences in summer.
690 The variability of ET_a of the individual lysimeters in relation to the lysimeter average was -7.9 to
691 3.1 % in 2012 with larger absolute differences in summer. Both ET_a -EC and ET_a -LYS were close
692 to the calculated Penman-Monteith evapotranspiration (ET_{PM}), which indicates that
693 evapotranspiration at the site was energy limited. The differences between ET_a -LYS, ET_a -EC and
694 ET_{PM} were mainly related to harvesting management at the study site. A relationship between
695 grass length at the lysimeter and differences between ET_{PM} and ET_a -LYS was found. Variable
696 grass cutting dates for different fields around the EC-station and the lysimeter harvest lead to
697 differences in actual evapotranspiration up to 2.1 mm day^{-1} for periods with larger grass length
698 discrepancies.

699 The correction of the energy balance deficit with the Bowen ratio method resulted in ET_a -EC
700 which was close to ET_a -LYS. If the correction was not applied, ET_a -EC was 16 % smaller than
701 for the case where it was applied. In contrast, if the EB-deficit was completely attributed to the
702 latent heat flux ET_a was 15.7 % larger than for the default case. These results point to the
703 importance of adequate EC data correction.

704 **Acknowledgements**

705 This research is based on data provided by the research infrastructures of TERENO and
706 TERENO-SoilCan. We thank the Transregio32 for contributing data from the Rollesbroich study
707 site and want to acknowledge H. Rützel, W. Benders, F. Engels, L. Fürst, W. Küppers, D. Dolfus,
708 and M. Kettler accounting for the realization and maintenance of the research facilities. We also
709 thank Andre Peters for providing the AWAT software. We further thank the "Arbeitskreis
710 Lysimeterdatenauswertung" for the stimulating discussions.

711 **References**

712 Akaike, H.: A new look at statistical model identification, *IEEE Transactions on Automatic*
713 *Control*, 19, 716–723, doi:10.1109/TAC.1974.1100705, 1974.

714 Alfieri, J. G., Kustas, W. P., Prueger, J. H., Hipps, L. E., Evett, S. R., Basara, J. B., Neale, C. M.
715 U., French, A. N., Colaizzi, P., Agam, N., Cosh, M. H., Chavez, J. L., and Howell, T. A.: On the
716 discrepancy between eddy covariance and lysimetry-based surface flux measurements under
717 strongly advective conditions, *Advances in Water Resources*, 50, 62-78,
718 doi:10.1016/j.advwatres.2012.07.008, 2012.

719 Allen, R. G., Pereira, L. S., Raes, D., Smith, M.: Crop evapotranspiration-Guidelines for
720 computing crop water requirements-FAO Irrigation and drainage paper 56. FAO, Rome, 9, 300,
721 1998.

722 Allen, R.G., Pruitt, W. O., Wright, J. L., Howell, T. A., Ventura, F., Snyder, R., Itenfisu, D.,
723 Steduto, P., Berengena, J., Yrisarry, J. B., Smith, M., Pereira, L. S., Raes, D., Perrier, A., Alves,
724 I., Walter, I., Elliott, R.: A recommendation on standardized surface resistance for hourly
725 calculation of reference ETo by the FAO56 Penman-Monteith method. *Agricultural Water*
726 *Management*, 81, 1-22, doi: 10.1016/j.agwat.2005.03.007, 2006.

727 Brutsaert, W.: *Hydrology: An Introduction* / Wilfried Brutsaert, 5th print. ed., Univ. Press,
728 Cambridge, XI, 605 S. pp., 2010.

729 Chávez, J., Howell, T., and Copeland, K.: Evaluating eddy covariance cotton ET measurements
730 in an advective environment with large weighing lysimeters, *Irrigation Science*, 28, 35-50,
731 doi:10.1007/s00271-009-0179-7, 2009.

732 Chvíla, B., Sevruk, B., and Ondrás, M.: The wind-induced loss of thunderstorm precipitation
733 measurements, *Atmospheric Research*, 77, 29-38, doi:10.1016/j.atmosres.2004.11.032, 2005.

734 Deutscher Wetterdienst (DWD): *Richtlinie für automatische Klimastationen*, Offenbach am
735 Main, 1993.

736 Ding, R., Kang, S., Li, F., Zhang, Y., Tong, L., and Sun, Q.: Evaluating eddy covariance method
737 by large-scale weighing lysimeter in a maize field of northwest China, *Agricultural Water*
738 *Management*, 98, 87-95, doi:10.1016/j.agwat.2010.08.001, 2010.

739 Evett, S. R., Schwartz, R. C., Howell, T. A., Louis Baumhardt, R., and Copeland, K. S.: Can
740 weighing lysimeter ET represent surrounding field ET well enough to test flux station
741 measurements of daily and sub-daily ET?, *Advances in Water Resources*, 50, 79-90,
742 doi:10.1016/j.advwatres.2012.07.023, 2012.

743 Feldhake, C. M. and Boyer, D. G.: Effect of soil temperature on evapotranspiration by C3 and C4
744 grasses, *Agricultural and Forest Meteorology*, 37, 309-318, doi:10.1016/0168-1923(86)90068-7,
745 1986.

746 Finnigan, J.: The footprint concept in complex terrain, *Agricultural and Forest Meteorology*, 127,
747 117-129, doi:10.1016/j.agrformet.2004.07.008, 2004.

748 Foken, T. and Wichura, B.: Tools for quality assessment of surface-based flux measurements,
749 *Agricultural and Forest Meteorology*, 78, 83-105, doi:10.1016/0168-1923(95)02248-1, 1996.

750 Foken, T.: The energy balance closure problem: An overview, *Ecological Applications*, 18, 1351-
751 1367, doi:10.1890/06-0922.1, 2008.

752 Foken, T., Aubinet, M., Finnigan, J. J., Leclerc, M. Y., Mauder, M., and Paw U, K. T.: Results Of
753 A Panel Discussion About The Energy Balance Closure Correction For Trace Gases, *Bulletin of*
754 *the American Meteorological Society*, 92, 13-18, doi:10.1175/2011bams3130.1, 2011.

755 Goodison, B. E., Louie, P. Y. T., and Yang, D.: The WMO solid precipitation measurement
756 intercomparison. *World Meteorological Organization-Publications-WMO TD*, 65-70, 1997.

757 Hendricks Franssen, H. J., R. Stöckli, I. Lehner, E. Rotenberg, and S. I. Seneviratne.: Energy
758 Balance Closure of Eddy-Covariance Data: A Multisite Analysis for European Fluxnet Stations,
759 *Agricultural and Forest Meteorology*, 150(12), 1553-1567, doi:10.1016/j.agrformet.2010.08.005,
760 2010.

761 Huang, W., Zhang, C., Xue, X., and Chen, L.: A Data Acquisition System Based on Outlier
762 Detection Method for Weighing Lysimeters, in: *Computer and Computing Technologies in*
763 *Agriculture V*, edited by: Li, D., and Chen, Y., *IFIP Advances in Information and*
764 *Communication Technology*, Springer Berlin Heidelberg, 471-478, 2012.

765 Hurvich, C. and Tsai, C.: Regression and time series model selection in small samples,
766 *Biometrika*, 76, 297–307, doi:10.1093/biomet/76.2.297, 1989.

767 Ingwersen, J., Steffens, K., Högy, P., Warrach-Sagi, K., Zhunusbayeva, D., Poltoradnev, M.,
768 Gäbler, R., Wizemann, H. D., Fangmeier, A., Wulfmeyer, V., and Streck, T.: Comparison of
769 Noah simulations with eddy covariance and soil water measurements at a winter wheat stand,
770 *Agricultural and Forest Meteorology*, 151, 345-355, doi: 10.1016/j.agrformet.2010.11.010, 2011.

771 Jacobs, A. F. G., Heusinkveld, B. G., Wichink Kruit, R. J., and Berkowicz, S. M.: Contribution of
772 dew to the water budget of a grassland area in the Netherlands, *Water Resources Research*, 42,
773 W03415, doi:10.1029/2005wr004055, 2006.

774 Kessomkiat, W., Hendricks Franssen, H. J., Graf, A., and Vereecken, H.: Estimating random
775 errors of eddy covariance data: An extended two-tower approach, *Agricultural and Forest*
776 *Meteorology*, 171–172, 203-219, doi:10.1016/j.agrformet.2012.11.019, 2013.

777 Kohnke, H., Davidson, J. M., and Dreibelbis, F. R.: A survey and discussion of lysimeters and a
778 bibliography on their construction and performance, U. S. Govt. print. off., Washington, D.C., 68
779 p., 1940.

780 Kormann, R. and Meixner, F.: An Analytical Footprint Model For Non-Neutral Stratification,
781 *Bound-Lay Meteorology*, 99, 207-224, doi:10.1023/a:1018991015119, 2001.

782 Legates, D. R. and DeLiberty, T. L.: Precipitation measurement biases in the United States,
783 *JAWRA Journal of the American Water Resources Association*, 29, 855-861, doi:10.1111/j.1752-
784 1688.1993.tb03245.x, 1993.

785 Li, S., Kang, S., Zhang, L., Li, F., Zhu, Z., and Zhang, B.: A comparison of three methods for
786 determining vineyard evapotranspiration in the arid desert regions of northwest China,
787 *Hydrological Processes*, 22, 4554-4564, doi:10.1002/hyp.7059, 2008.

788 López-Urrea, R., Olalla, F. M. d. S., Fabeiro, C., and Moratalla, A.: An evaluation of two hourly
789 reference evapotranspiration equations for semiarid conditions, *Agricultural Water Management*,
790 86, 277-282, doi:10.1016/j.agwat.2006.05.017, 2006.

791 Mauder, M. and Foken, T.: Documentation and Instruction Manual of the Eddy-Covariance
792 Software Package TK3. Arbeitsergebnisse / Universität Bayreuth, Abteilung Mikrometeorologie,
793 2011.

794 Mauder, M., Cuntz, M., Drüe, C., Graf, A., Rebmann, C., Schmid, H. P., Schmidt, M., and
795 Steinbrecher, R.: A strategy for quality and uncertainty assessment of long-term eddy-covariance
796 measurements, *Agricultural and Forest Meteorology*, 169, 122-135,
797 doi:10.1016/j.agrformet.2012.09.006, 2013.

798 Meissner, R., Seeger, J., Rupp, H., Seyfarth, M., and Borg, H.: Measurement of dew, fog, and
799 rime with a high-precision gravitation lysimeter, *Journal of Plant Nutrition and Soil Science*, 170,
800 335-344, doi:10.1002/jpln.200625002, 2007.

801 Michelson, D. B.: Systematic correction of precipitation gauge observations using analyzed
802 meteorological variables, *Journal of Hydrology*, 290, 161-177,
803 doi:10.1016/j.jhydrol.2003.10.005, 2004.

804 Moore, C.J.: Frequency response corrections for eddy correlation systems. *Boundary-Layer*
805 *Meteorology*, 37, 17-35, doi: 10.1007/bf00122754, 1986.

806 Nešpor, V. and Sevruk, B.: Estimation of Wind-Induced Error of Rainfall Gauge Measurements
807 Using a Numerical Simulation, *Journal of Atmospheric and Oceanic Technology*, 16, 450-464,
808 10.1175/1520-0426(1999)016<0450:eowieo>2.0.co;2, 1999.

809 Nolz, R., Kammerer, G., and Cepuder, P.: Interpretation of lysimeter weighing data affected by
810 wind, *Journal of Plant Nutrition and Soil Science*, 176, 200–208, doi:10.1002/jpln.201200342,
811 2013.

812 Peters, A., Nehls, T., Schonsky, H., and Wessolek, G.: Separating precipitation and
813 evapotranspiration from noise - a new filter routine for high-resolution lysimeter data, *Hydrology*
814 *and Earth System Sciences*, 18, 1189-1198, doi:10.5194/hess-18-1189-2014, 2014.

815 Qu, W., Bogena, H. R., Huisman, J. A., and Vereecken, H.: Calibration of a Novel Low-Cost Soil
816 Water Content Sensor Based on a Ring Oscillator, *Vadose Zone Journal*, 12, 3,
817 doi:10.2136/vzj2012.0139, 2013.

818 Richter, D.: Ergebnisse methodischer Untersuchungen zur Korrektur des systematischen
819 Messfehlers des Hellmann-Niederschlagsmessers *Berichte des Deutschen Wetterdienstes*, 194,
820 1995.

821 Savitzky, A. and Golay, M.: Smoothing and Differentiation of Data by Simplified Least Squares
822 Procedures, *Analytical Chemistry*, 36, 1627–1639, doi:10.1021/ac60214a047, 1964.

823 Schrader, F., Durner, W., Fank, J., Gebler, S., Pütz, T., Hannes, M., and Wollschläger, U.:
824 Estimating Precipitation and Actual Evapotranspiration from Precision Lysimeter Measurements,
825 *Procedia Environmental Sciences*, 19, 543-552, doi:10.1016/j.proenv.2013.06.061, 2013.

826 Schotanus, P., Nieuwstadt, F. T. M., de Bruin, H. A. R.: Temperature measurement with a sonic
827 anemometer and its application to heat and moisture fluxes. *Boundary-Layer Meteorology* 26,
828 81-93, doi:10.1007/bf00164332, 1983.

829 Scott, R. L.: Using watershed water balance to evaluate the accuracy of eddy covariance
830 evaporation measurements for three semiarid ecosystems, In: *Agricultural and Forest*
831 *Meteorology*, 150(2), 219-225, doi:10.1016/j.agrformet.2009.11.002, 2010.

832 Sevruk, B.: Methodische Untersuchungen des systematischen Messfehlers der Hellmann-
833 Regenmesser im Sommerhalbjahr in der Schweiz. *Mitteilungen Nr. 52*, Versuchsanstalt für
834 Wasserbau, Hydrologie und Glaziologie, ETH Zürich, 299 Book pp., 1981.

835 Sevruk, B.: Wind induced measurement error for high-intensity rains. *Proc. International*
836 *Workshop on Precipitation Measurement*, WMO Tech. Document 328, St. Moritz, Switzerland,
837 199–204, 1989.

838 Sevruk, B.: Adjustment of tipping-bucket precipitation gauge measurements, *Atmospheric*
839 *Research*, 42, 237-246, doi:10.1016/0169-8095(95)00066-6, 1996.

840 Strangeways, I.: A history of rain gauges, *Weather*, 65, 133-138, 10.1002/wea.548, 2010.

841 Twine, T. E., Kustas, W. P., Norman, J. M., Cook, D. R., Houser, P. R., Meyers, T. P., Prueger, J.
842 H., Starks, P. J., and Wesely, M. L.: Correcting eddy-covariance flux underestimates over a
843 grassland, *Agricultural and Forest Meteorology*, 103, 279-300, doi:10.1016/S0168-
844 1923(00)00123-4, 2000.

845 Unold, G. and Fank, J.: Modular Design of Field Lysimeters for Specific Application Needs,
846 *Water Air Soil Pollution, Focus*, 8, 233-242, doi:10.1007/s11267-007-9172-4, 2008.

847 Vaughan, P. J., Trout, T. J., and Ayars, J. E.: A processing method for weighing lysimeter data
848 and comparison to micrometeorological ET_0 predictions, *Agricultural Water Management*, 88,
849 141-146, doi:10.1016/j.agwat.2006.10.008, 2007.

850 Vaughan, P. J. and Ayars, J.: Noise Reduction Methods for Weighing Lysimeters, *Journal of*
851 *Irrigation and Drainage Engineering*, 135, 235-240, doi:10.1061/(ASCE)0733-
852 9437(2009)135:2(235), 2009.

853 Webb, E. K., Pearman ,G. I., Leuning, R.: Correction of flux measurements for density effects
854 due to heat and water vapour transfer, *Quarterly Journal of the Royal Meteorological Society*,
855 106, 85-100, doi:10.1002/qj.49710644707, 1980.

856 Wegehenkel, M. and Gerke, H. H.: Comparison of real evapotranspiration measured by weighing
857 lysimeters with simulations based on the Penman formula and a crop growth model, *Journal of*
858 *Hydrology and Hydromechanics*, 61, 161–172, doi:10.2478/johh-2013-0021, 2013.

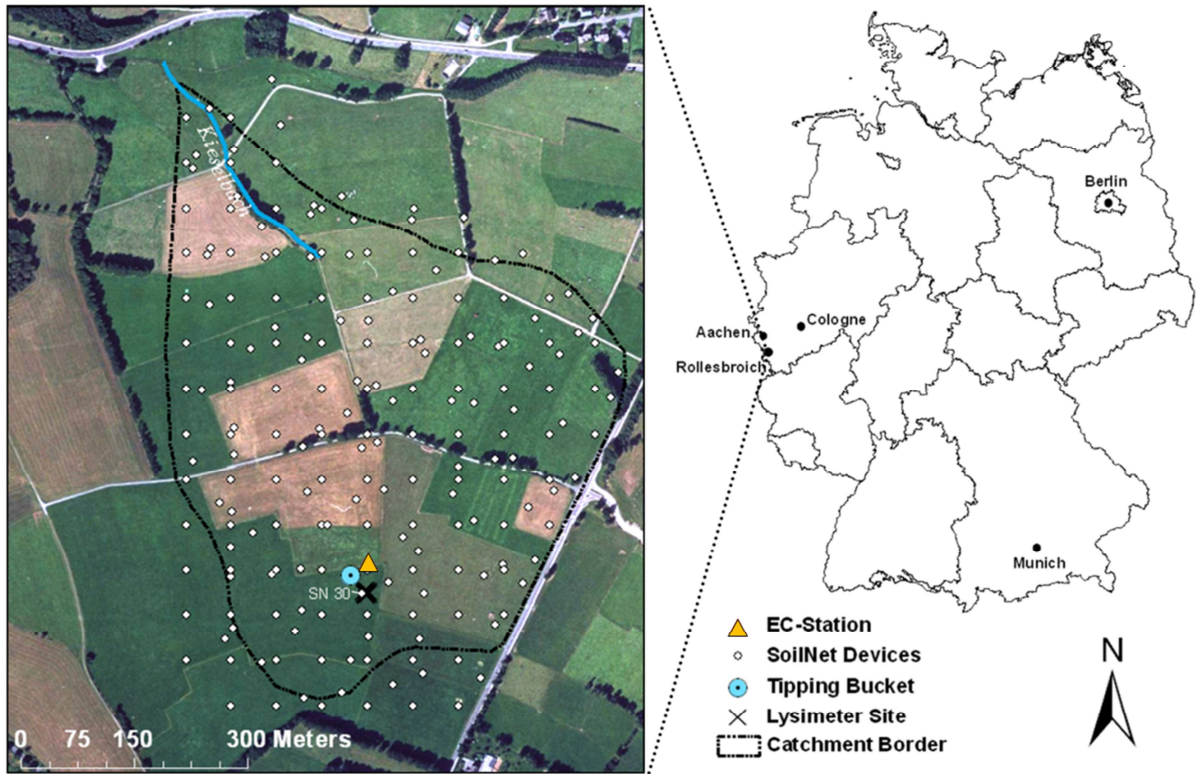
859 Wilczak, J., Oncley, S., and Stage, S.: Sonic Anemometer Tilt Correction Algorithms, *Bound-*
860 *Layer Meteorology*, 99, 127-150, doi:10.1023/a:1018966204465, 2001.

861 Wilson, K. B., Hanson, P. J., Mulholland, P. J., Baldocchi, D. D., and Wullschleger, S. D.: A
862 comparison of methods for determining forest evapotranspiration and its components: sap-flow,
863 soil water budget, eddy covariance and catchment water balance, *Agricultural and Forest*
864 *Meteorology*, 106, 153-168, doi:10.1016/S0168-1923(00)00199-4, 2001.

865 Yang, D., Goodison, B. E., Metcalfe, J. R., Golubev, V. S., Bates, R., Pangburn, T., and Hanson,
866 C. L.: Accuracy of NWS 8" Standard Nonrecording Precipitation Gauge: Results and Application
867 of WMO Intercomparison, *Journal of Atmospheric and Oceanic Technology*, 15, 54-68,
868 doi:10.1175/1520-0426(1998)015<0054:AONSNP>2.0.CO;2, 1998.

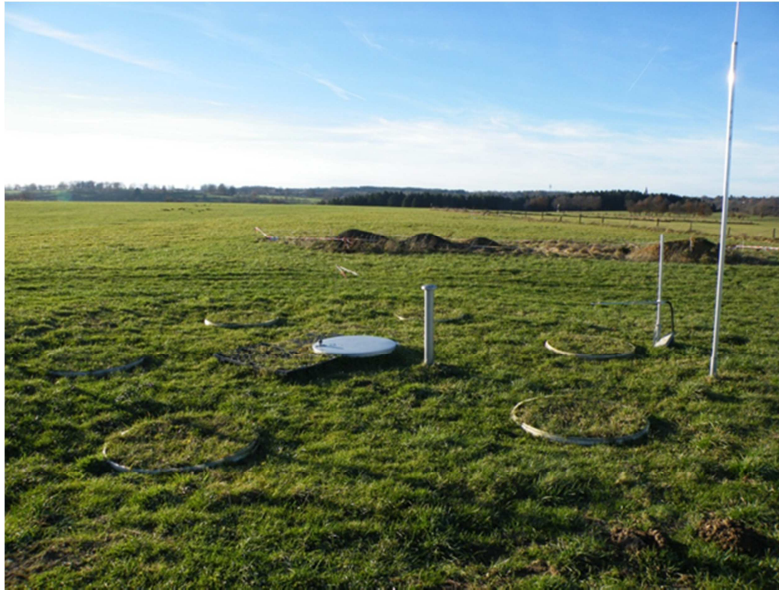
869 Zacharias, S., Bogen, H., Samaniego, L., Mauder, M., Fuß, R., Pütz, T., Frenzel, M., Schwank,
870 M., Baessler, C., Butterbach-Bahl, K., Bens, O., Borg, E., Brauer, A., Dietrich, P., Hajnsek, I.,
871 Helle, G., Kiese, R., Kunstmann, H., Klotz, S., Munch, J. C., Papen, H., Priesack, E., Schmid, H.
872 P., Steinbrecher, R., Rosenbaum, U., Teutsch, G., and Vereecken, H.: A Network of Terrestrial
873 Environmental Observatories in Germany, *Vadose Zone Journal*, 10, 955-973,
874 doi:10.2136/vzj2010.0139, 2011.

875 Zenker, T.: Verdunstungswiderstände und Gras-Referenzverdunstung : Lysimeteruntersuchungen
876 zum Penman-Monteith-Ansatz im Berliner Raum. PhD thesis, Berlin University of Technology,
877 Germany, 2003.



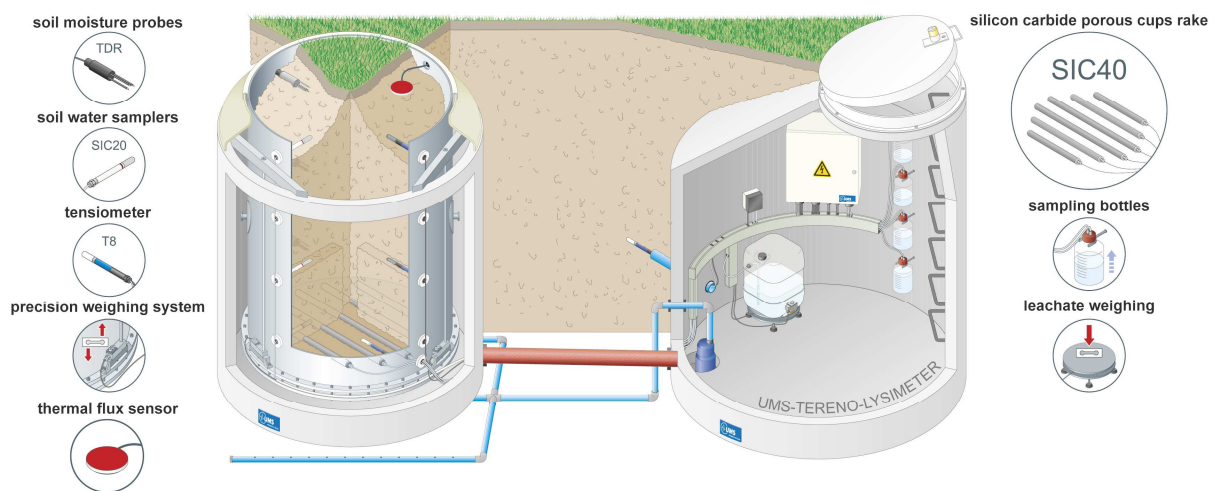
879

880 **Fig. 1.** Overview of the Rollesbroich study site (left) showing the locations of the lysimeter, the
 881 rain gauge, the eddy covariance station, the catchment boundaries and the SoilNet devices. All
 882 devices are arranged within a radius of 50 meters including the nearest SoilNet device (SN 30)
 883 for comparison of temperature and soil water content with the surrounding field. The map on the
 884 right shows the location of the Rollesbroich catchment in Germany.



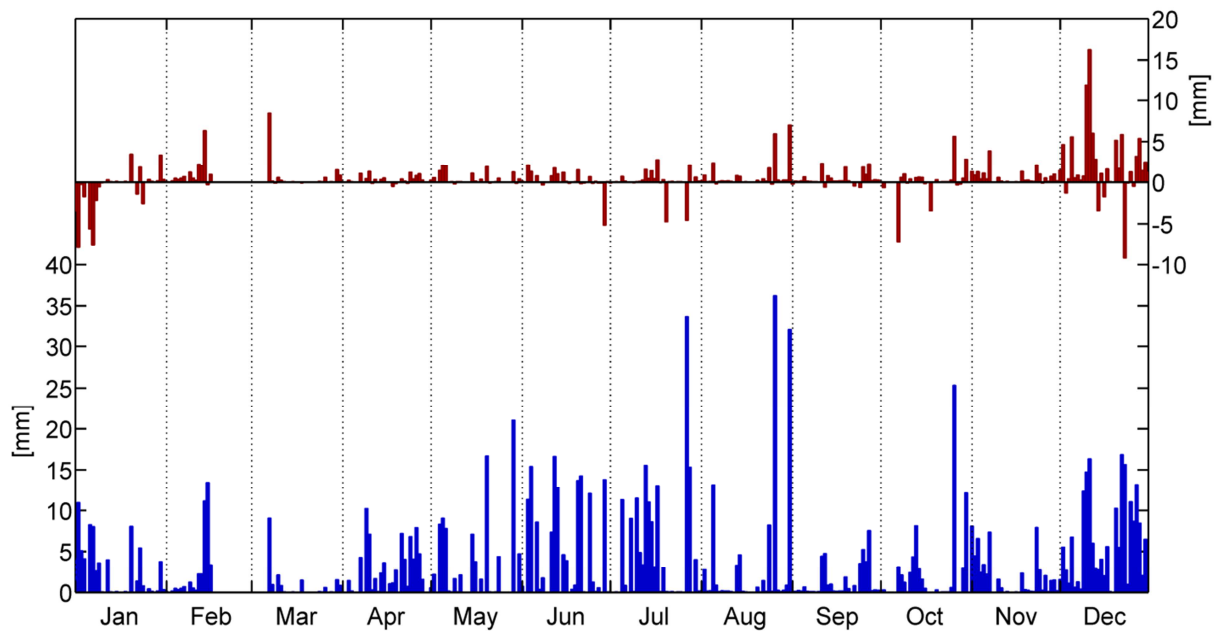
885

886 **Fig. 2.** The lysimeter set-up of the Rollesbroich study site (November 2012).



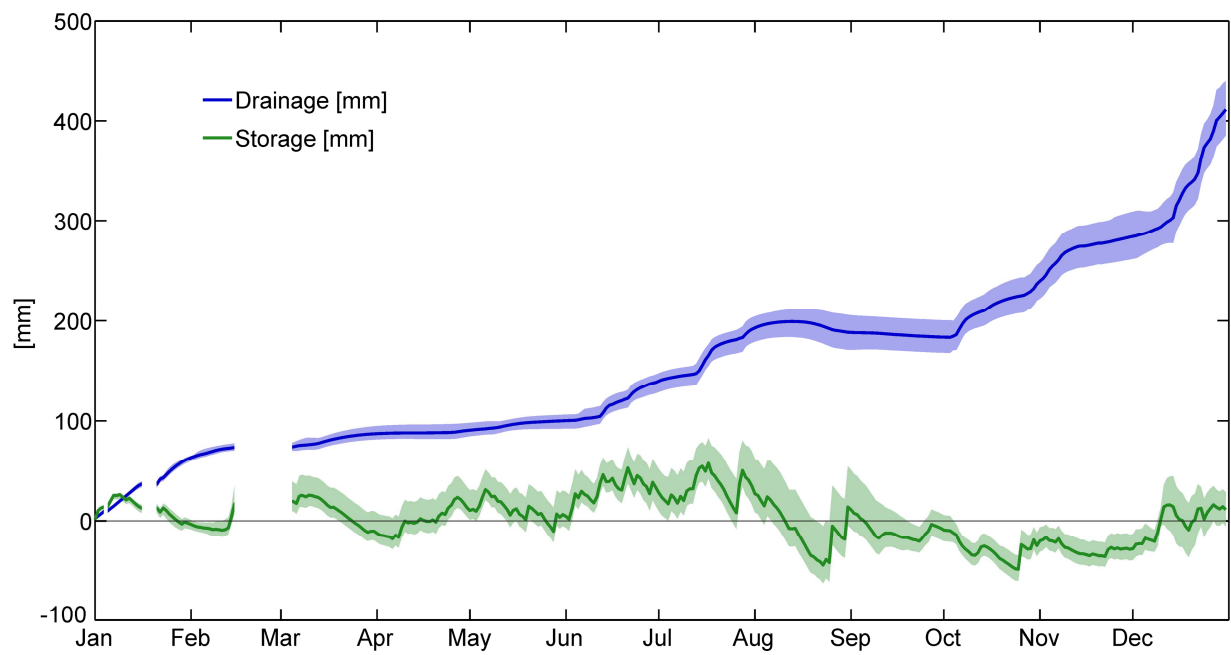
887

888 **Fig. 3.** Schematic drawing of the lysimeter soil monolith (left) and service well (right) used in the
 889 TERENO-SoilCan project. The illustration of the lysimeter (left) shows the weighted soil column
 890 container with slots for soil moisture (TDR), temperature (SIS, TS1), matric potential sensors
 891 (SIS), soil water sampler (SIC20) and silicon porous suction cup rake (SIC40) installation inside
 892 and outside the monolith. The service well contains the weighted drainage tank and sampling
 893 tubes for each affiliated lysimeter (courtesy of UMS GmbH Munich, 2014, used by permission).

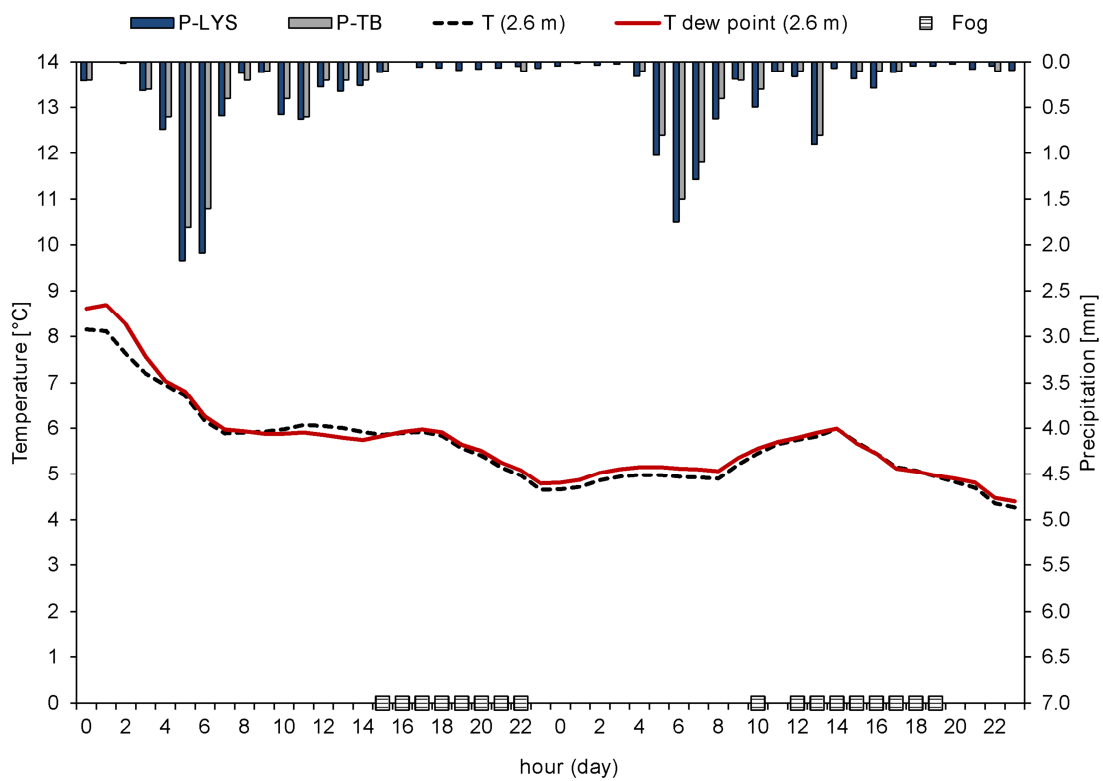


894

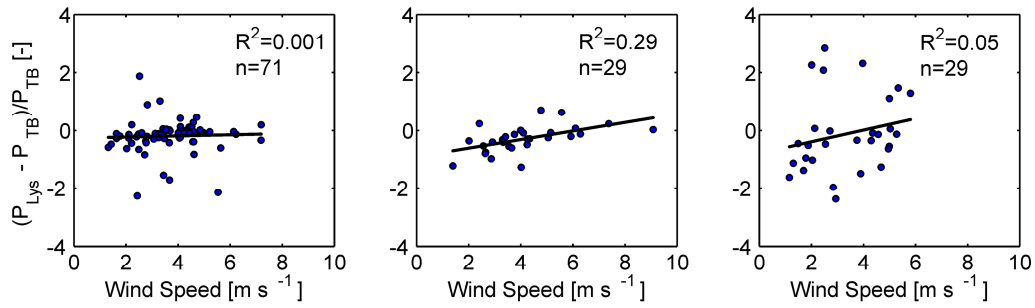
895 **Fig. 4.** Daily precipitation sums of tipping bucket (blue) and difference in precipitation
 896 measurements between lysimeter and TB (red) at the Rollesbroich study site for 2012.



897
 898 **Fig. 5.** Cumulated average of lysimeter drainage and soil moisture storage on a daily basis. The
 899 colored areas indicate the range of minimum and maximum cumulated drainage and soil water
 900 storage for the individual lysimeters.

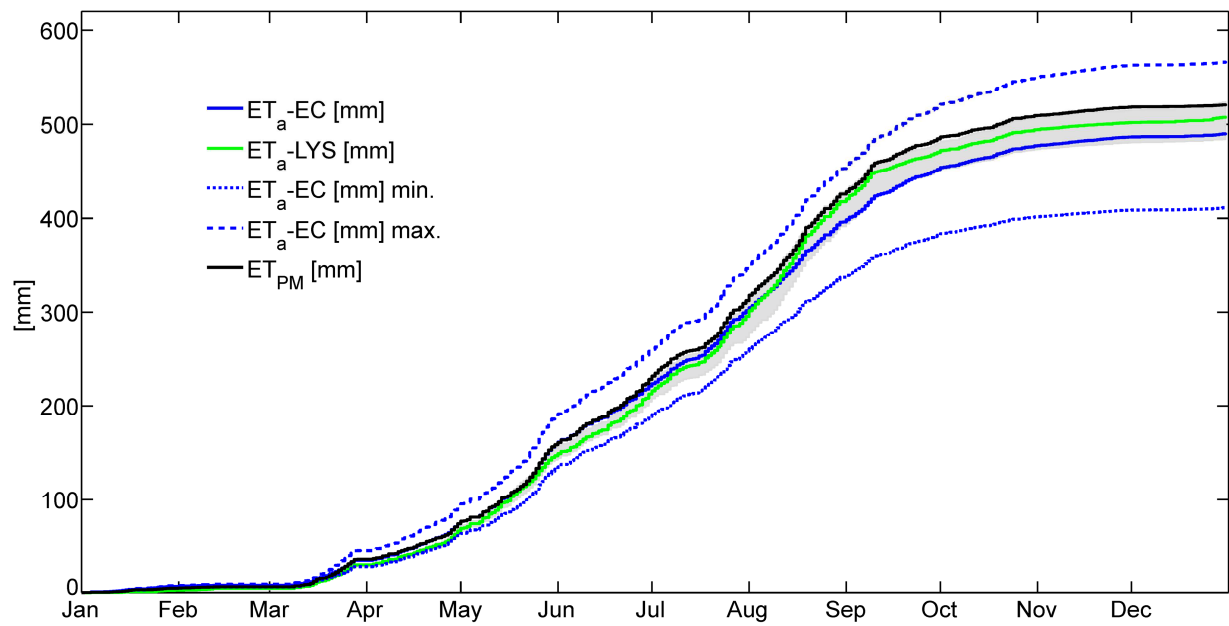


901
 902 **Fig. 6.** Precipitation, temperature and dew point temperature from May 5 – May 6 2012 at the
 903 Rollesbroich site. The fog symbol indicates the hours with fog occurrence (detected with installed
 904 surveillance system) for the investigated period.



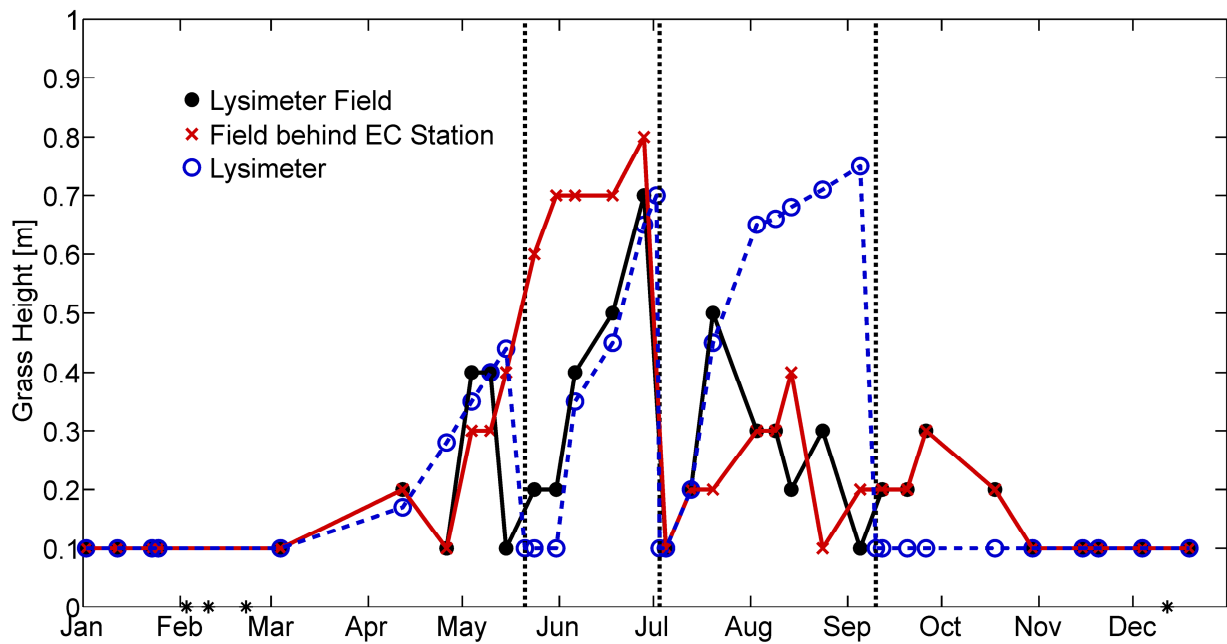
905

906 **Fig. 7.** Relationship between wind speed and precipitation residuals relative to TB precipitation
 907 on a daily basis. The relationships are classified according precipitation intensities of 1-5 mm
 908 (a), 5-10 mm (b), and > 10 mm (c). Potential rime and dew situation are excluded from the
 909 calculation.



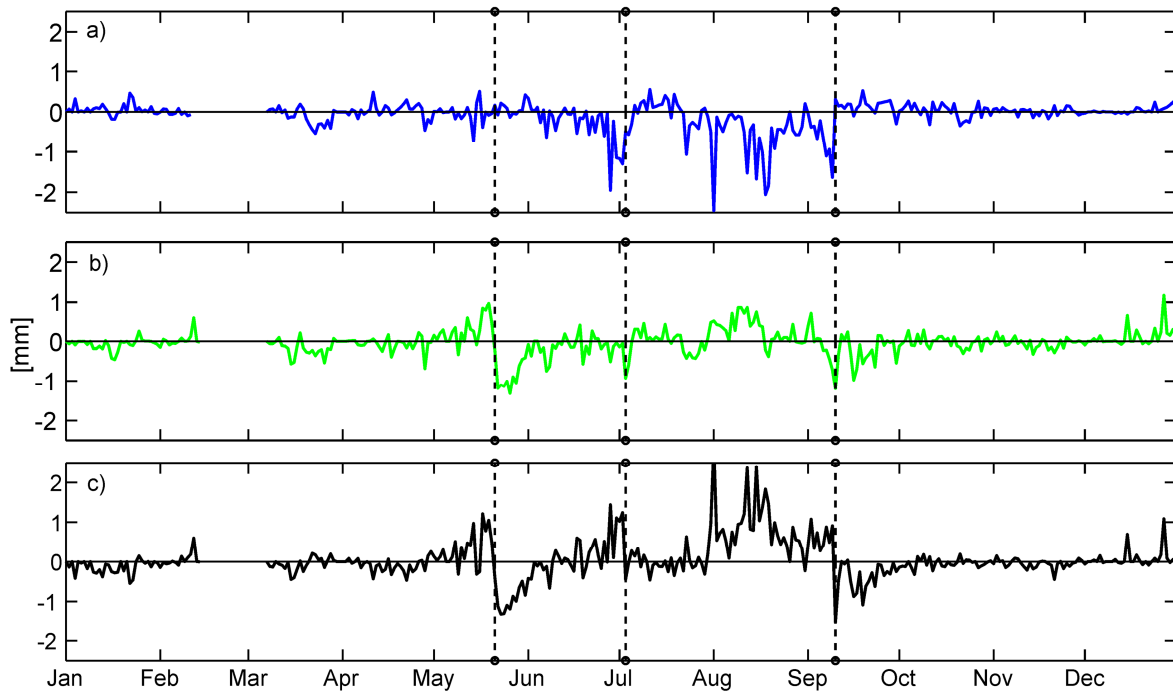
910

911 **Fig. 8.** Cumulative ET_a -LYS, ET_a -EC (corrected according to Bowen ratio), ET_{PM} on hourly
 912 basis for 2012. Displayed are also ET_a -EC max. and ET_a -EC min. The area in grey shows the
 913 range of minimum and maximum cumulated ET_a for the individual lysimeters.



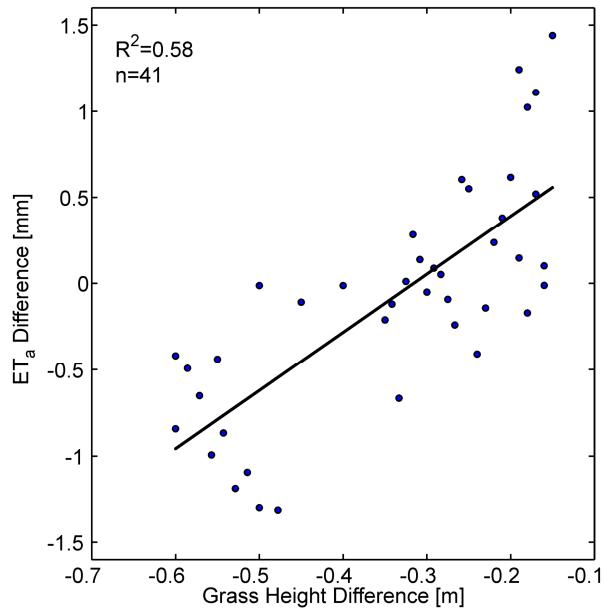
914

915 **Fig. 9.** Grass heights at the lysimeter field, the lysimeter devices, and the field behind the EC
 916 station for 2012. The grass length at the lysimeter devices was reconstructed by comparing grass
 917 length measurements of the lysimeter field with the observations of the surveillance system. The
 918 star (*) indicates the presence of a snow cover. Grass cutting dates on lysimeter devices are
 919 marked by dashed lines.



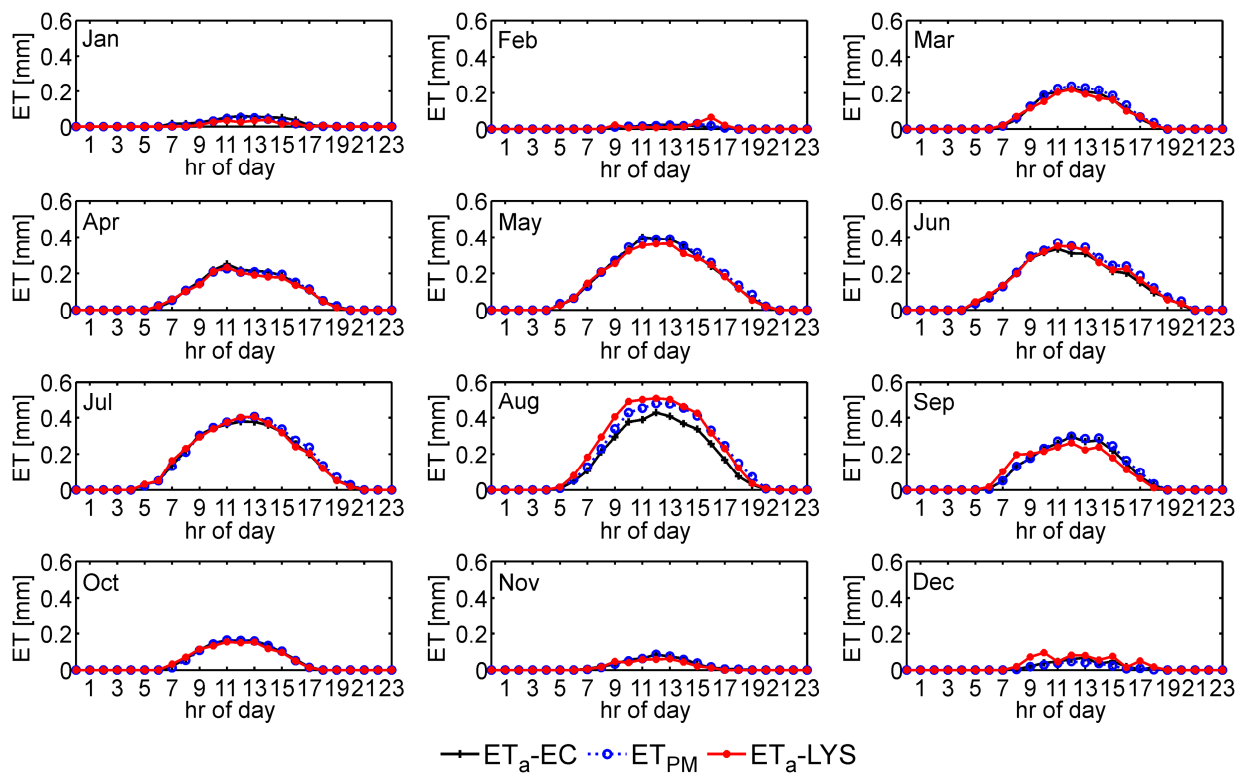
920

921 **Fig. 10.** Differences between daily ET for 2012. Displayed are $ET_a-EC - ET_{PM}$ (a), $ET_a-LYS -$
 922 ET_{PM} (b) and $ET_a-LYS - ET_a-EC$ (c). The dashed lines indicate harvest at lysimeters.

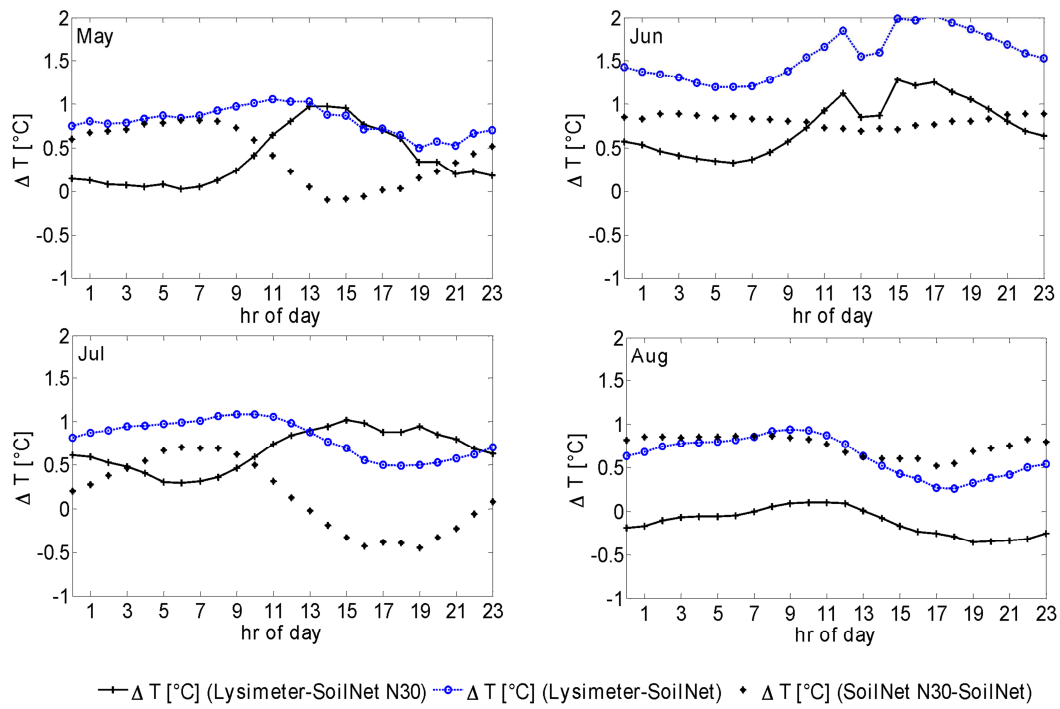


923

924 **Fig. 11.** Relationship between grass length difference (between the lysimeters and the field
925 behind the EC-device) and ET_a difference measured by lysimeters and EC station from May 21 –
926 July 3.



928 **Fig. 12.** Mean daily cycle of ET_a -LYS, ET_a -EC and ET_{PM} for 2012.



929

930 **Fig. 13.** Differences in daily mean soil temperature (averaged over the six lysimeters), a nearby
 931 SoilNet device (SN 30) and the mean of all available SoilNet devices located at the study site.

932 **Tables**

933 **Tab. 1.** Site specific wind exposition coefficient b [-] and empiric precipitation type coefficient
934 ϵ [-] for different precipitation types at an open space gauge location.

Precipitation Type	b	ϵ
liquid (summer)	0.345	0.38
liquid (winter)	0.34	0.46
mixed	0.535	0.55
snow	0.72	0.82

935 **Tab. 2.** Monthly precipitation sums for lysimeter, tipping bucket, corrected tipping bucket data and a comparison between the hourly
 936 precipitation values of lysimeter and uncorrected TB in terms of coefficient of determination (R^2), root mean square error and other
 937 statistics at the Rollesbroich study site for 2012. Missing data % refers to the percentage of hourly precipitation data not available for
 938 comparison.

Month	Lysimeter Average [mm]	Min. / Max. Lysimeter [mm]	Tipping Bucket [mm]	Tipping Bucket corrected [mm]	R^2	RMSE	LYS/TB %	LYS/ TBcorr %	Missing Data %
Jan	70.9	57.6 / 79.3	94.0	110.7	0.48	0.30	75.6	64.0	11.2
Feb	36.2	31.4 / 48.9	21.1	26.0	0.13	0.32	171.6	139.2	46.1
Mar	17.3	16.2 / 18.8	5.1	7.3	0.18	0.16	339.2	237.0	16.4
Apr	72.5	71.1 / 74.6	65.3	78.2	0.90	0.09	111.0	92.7	0.0
May	90.7	89.4 / 94.1	79.3	88.8	0.99	0.09	114.4	114.4	0.0
Jun	139.9	137.5 / 143.1	134.7	147.2	0.96	0.21	103.9	95.0	0.0
Jul	148.5	146.3 / 152.2	147.0	159.2	0.95	0.28	101.0	93.3	0.0
Aug	105.7	100.4 / 109.4	84.5	91.9	0.94	0.15	125.1	115.0	0.0
Sep	36.5	23.5 / 39.2	25.6	30.5	0.58	0.13	142.6	119.7	0.0
Oct	67.5	65.7 / 69.5	66.2	75.2	0.74	0.23	102.0	89.8	13.4
Nov	55.3	52.7 / 56.9	38.3	45.8	0.84	0.08	144.4	120.7	0.0
Dec	186.0	178.5 / 194.4	121.0	136.1	0.30	0.35	153.7	136.7	0.0
SUM /MEAN	1027.1	996.2 / 1037.7	882.1	996.9	0.88	0.47	116.4	103.0	7.1

939

940 **Tab. 3.** Monthly ET_a (by lysimeter and EC), ET_{PM} sums and R^2 between different ET data products on an hourly basis for 2012. Missing
 941 data % refers to the percentage of hourly ET data (ET_a -EC, ET_a -LYS) between sunrise und sunset not available for comparison. Hence,
 942 the total yearly ET amount is ca. 18 % reduced compared to gap free ET estimations.

	2012												Sum	Mean
	Jan	Feb	Mar	Apr	May	Jun	Jul	Aug	Sep	Oct	Nov	Dec		
ET_a-EC [mm]	5.2	1.3	27.8	38.4	84.3	62.7	80.3	94.2	56.0	25.2	9.3	3.6	488.3	
ET_{PM} [mm]	3.9	1.5	30.5	37.5	84.2	69.7	84.0	113.5	58.9	24.6	9.0	2.5	519.8	
ET_a-LYS [mm]	2.5	2.2	26.4	35.6	80.2	65.7	82.7	121.7	52.7	23.9	7.6	5.9	507.4	
Min. / Max.	2.1 /	1.3 /	25.9 /	34.4 /	75.2 /	62.1 /	67.8 /	116.8 /	49.6 /	21.9 /	6.8 /	3.0 /	467.1 /	
ET_a-LYS [mm]	2.7	3.1	26.8	37.6	85.2	68.2	91.0	125.2	58.8	27.1	8.9	8.7	523.1	
R^2 ET_a-EC - ET_a-LYS	0.02	0.02	0.82	0.76	0.79	0.84	0.86	0.86	0.66	0.66	0.39	0.06		0.81
R^2 ET_a-LYS - ET_{PM}	0.13	0.00	0.87	0.82	0.86	0.91	0.89	0.92	0.78	0.70	0.41	0.08		0.89
R^2 ET_a-EC - ET_{PM}	0.12	0.00	0.94	0.93	0.95	0.90	0.89	0.88	0.88	0.82	0.73	0.44		0.91
Missing Data %	33.2	36.9	8.1	23.5	21.5	26.5	21.9	12.9	14.0	25.8	25.0	45.3	24.5	

1 **Tab. 4.** Measured mean monthly latent heat fluxes and corrections for EBD for 2012.

Month	Mean LE [W m⁻¹]	Mean LE corr. [W m⁻¹]	Differences LE corr. - LE	Difference mean LE corr. - LE %
Jan	21.9	29.8	7.9	36.2
Feb	8.7	11.9	3.2	36.9
Mar	78.1	94.0	15.9	20.4
Apr	86.4	101.8	15.3	17.7
May	138.7	164.6	25.9	18.7
Jun	111.8	125.8	14.0	12.6
Jul	136.3	157.2	20.9	15.3
Aug	151.6	181.4	29.8	19.6
Sep	104.0	129.2	25.2	24.2
Oct	61.3	79.6	18.3	29.9
Nov	24.4	32.1	7.7	31.4
Dec	22.0	28.3	6.3	28.5
SUM/MEAN	78.8	94.6	15.9	24.3

2